Identifying Targetable Liabilities in Ewing Sarcoma

Abstract:

Background: Despite multi-modality therapy, the majority of patients with metastatic or recurrent Ewing sarcoma (ES), the second most common pediatric bone malignancy, will die of their disease. ES tumors express aberrantly activated ETS transcription factors through translocations that fuse the *EWS* gene to *ETS* family genes *FLI1* or *ERG*. The aberrant activation of *ETS* transcription factors promotes malignant transformation and proliferation. While, FLI1 or ERG cannot be readily targeted, there is an opportunity to deploy functional genomics screens, to develop novel therapeutic approaches by identifying targetable liabilities in *EWS/FLI1* dependent tumors.

Materials and Methods: We performed a near whole-genome pooled shRNA screen in a panel of five *EWS/FLI1* dependent Ewing sarcoma cell lines and one *EWS/ERG* cell line to identify essential genes. Essential genes were defined as those genes whose loss resulted in reduced viability selectively in ES cells compared to non-Ewing cancer cell lines. Essential hits were subsequently validated with genomic knockdown and chemical inhibition *in vitro,* followed by validation of the on-target effect of chemical inhibition. Next, we determined the *in vivo* effects of small-molecule inhibition on survival and tumor growth in NOD scid gamma (NSG) mice with established subcutaneous ES xenografts.

Results: Top hits in our screen that could be readily targeted by small-molecule inhibitors, and thus have potential for rapid clinical validation, were selected for further investigation. These hits included IKBKE, CCND1 and CDK4. IKBKE, a non-canonical IKK with an oncogenic role in breast cancer, was one of the top kinase hits in the screen. IKBKE shares significant homology to TBK1, another non-canonical IKK that is essential in k-RAS dependent lung cancer. We validated IKBKE through small-molecule inhibition of IKBKE/TBK1 and shRNA based knockdown. Ewing sarcoma cell lines are sensitive to low micromolar concentrations of

two IKBKE/TBK1 inhibitors (CYT387 and MRT67307). Additionally, in a panel of ES cell lines, knockdown of IKBKE resulted in decreased growth and impaired colony formation. These observations, paired with impairment of NF-κB nuclear localization following CYT387 treatment suggests that non-canonical IKK mediated signaling may be essential in Ewing sarcoma. We further validated these results through inhibition of IKBKE/TBK1 in *in vivo* xenograft models treated with 100 mg/kg/day of CYT387. Treatment over the course of twenty-nine days resulted in a significant increase in survival (p-value = 0.0231) and a significant decrease (p-value = 0.036) in tumor size after fifteen days of treatment.

CDK4 and CCND1 are highly expressed in Ewing sarcoma as compared to other tumor types. shRNA mediated knockdown of CDK4 and CCND1 resulted in impaired viability and anchorage independent growth. Furthermore, treatment of Ewing sarcoma cell lines with a highly selective CDK4/6 inhibitor, LEE011, resulted in decreased viability (IC_{50} range of 0.26-18.06 μM), potent G1 arrest in six of eight EWS/FLI1 containing Ewing sarcoma lines tested and apoptosis in a panel of four highly sensitive lines. Administration of 75 mg/kg/day and 250 mg/kg/day of LEE011 in NSG mice with Ewing xenografts resulted in significant impairment of tumor growth, (p-value <0.001 for both treatment arms), as compared to vehicle control.

Conclusions: These studies suggest a role for the targeting of IKBKE and CDK 4/6 in Ewing sarcoma, findings with immediate clinical relevance for patients with this malignancy, because small-molecule inhibitors of these proteins have already entered clinical trial for other disease indications.

Table of Contents:

Glossary of abbreviations:

Akt: also known as protein kinase B

ATP: Adenosine triphosphate

CCND1: Cyclin D1

CDK4: Cyclin-dependent kinase 4

CD99: Cluster of differentiation 99, also known as MIC2

CYLD: cylindromatosis gene

cIAP: cellular Inhibitor of Apoptosis

EFT: Ewing sarcoma family of tumors

ERG: *ETS*-related gene

ES: Ewing sarcoma

ETS: E26 Transformation-specific transcription factor or Erythroblast transformation-specific transcription factor

EWS: Ewing sarcoma gene

FLI1: Friend leukemia integration 1 transcription factor, also known as transcription factor ERGB

IC_{50}: Fifty percent inhibitory concentration

ID2: Inhibitor of DNA binding 2

IκBα: Inhibitor of kappa B (κB)

IKBKA: Inhibitor of kappa B (κB) kinase alpha, also known as IKKα

IKBKB: Inhibitor of kappa B (κB) kinase beta, also known as IKKβ

IKBKE: Inhibitor of kappa B (κB)kinase epsilon, also known as IKKε or IKK-i

IKK: Inhibitor of kappa B (κB) kinase

MEF: Mouse embryonic fibroblasts

NF-κB: Nuclear factor-kappa B (κB)

NKX2.2: NK2 Homeobox 2

NR0B1: Nuclear Receptor Subfamily 0, Group B, Member 1, also known as DAX-1

NSG: Nod-SCID-gamma mice

PARP-1: Poly [ADP-ribose] polymerase 1, also known as NAD+ ADP-ribosyltransferase 1

PI: Propidium iodide

RPM: Revolutions per minute

shRNA: small hairpin RNA

TANK: TRAF family member NF-κB activator

TBK1: TANK-binding kinase 1

TRAF2: TNF receptor associated factor 2

TRAF6: TNF receptor associated factor 6

Introduction

Ewing sarcoma (ES) is the second most common pediatric bone malignancy in the United States. Despite advances in treatment of primary ES, the disease continues to have very poor survival for patients with metastatic or relapsed disease, even with multi-modality therapy.[1,2]

ES represents a spectrum of tumors belonging to Ewing sarcoma family of tumors (EFT). These tumors are often located in diaphyses of long bones and appear as undifferentiated "small round blue cells" on histological examination. EFT also include chest wall tumors (Askin tumors) and atypical ES.[3] EFT share similarities not only in histology, but also in molecular biology, as they are characterized by balanced chromosomal translocations that define the biology of the disease.[4] Characteristic translocations involve fusion of *EWS* with *ETS* transcription factor-encoding genes. The most common translocation, present in 85% of Ewing sarcoma, involves chromosome t(11;22) which results in the fusion of the *5'* end of the transcriptional regulator encoding gene *EWS* with the *3'* region of the transcription factor encoding gene *FLI1*.[5] The resultant, aberrantly expressed 72-kDa-fusion protein is a nuclear protein that retains DNA-binding activity, recognizing the GGAA Ets- family DNA binding site.[6] Another 5-10% of ES and related tumors can also arise from a second chromosome translocation, t(21;22), that fuses *EWS* with the *ETS* family transcription factor encoding gene *ERG*, resulting in the fusion protein (EWS/ERG).[7]

EWS/FLI1 promotes transformation and tumorigenesis in Ewing sarcoma

EWS/FLI1 expression is oncogenic with cDNA transcripts of EWS/FLI1 capable of transforming NIH-3T3 cells, while absence of the EWS or FLI1 domain from the cDNA transcript abrogates this phenotype.[8] NIH-3T3 cells that express EWS/FLI1 result in accelerated tumor formation in immunocompromised mice. Additionally, dominant negative and RNA interference studies have demonstrated a dependence of Ewing sarcoma cells on the EWS/FLI1

fusion protein.[9,10] The fusion of EWS/FLI1 results in an aberrant transcription profile in which the N-terminal EWS domain promotes greater transcriptional activation than the native FLI1 protein alone and the intact DNA-binding domain of FLI1 within EWS/FLI1 results in localization of the protein to GGAA containing promoter or enhancer sites on target genes.[11]

Targets of EWS/FLI1 as mediators of Ewing sarcoma oncogenesis

Several targets of EWS/FLI1 have been identified and among these regulated genes, some have been shown to promote the oncogenic phenotype of Ewing sarcoma. For example, EWS/FLI1 expression results in overall gene downregulation that has been attributed to the direct activation of transcriptional repressors, such as NKX2.2 and NR0B1, by EWS/FLI1.[9,12,13] Additional direct targets of EWS/FLI1 that play a role in ES oncogenesis include the cell surface marker CD99 and inhibitor of DNA binding 2 (ID2). CD99, also known as MIC2, is a 32 kDa integral membrane glycoprotein that is used as a histologic marker for the diagnosis of Ewing sarcoma. It has been shown to be essential for Ewing transformation, with decreased expression of CD99 in patient derived Ewing cells resulting in abrogation of the transformation phenotype. The knockdown of CD99 also inhibits neural differentiation and results in G2 arrest with an increase in apoptosis.[14] ID2 has been shown to be upregulated in several tumor types including colon and pancreatic adenocarcinoma as well as neuroblastoma. The upregulation of ID2 in these tumor types is mediated by c-Myc, N-myc or β-catenin, while it has been linked to EWS/FLI1 in ES. Functionally, ID2 acts as an antagonist of basic helix-loop-helix proteins and regulates the switch between cell proliferation and differentiation.[15]

Aberrations in G1 checkpoint regulation in Ewing sarcoma

Another important target of EWS/FLI1 mediated transformation in cyclin D1. EWS/FLI1 has been shown to regulate cyclin D1 expression with inhibition of EWS/FLI1 resulting in a decrease of cyclin D1 and an increase of cyclin D3. The induction of EWS/FLI1 in a

rhabdomyosarcoma cell background, which classically has increased cyclin D3 and an absence of cyclin D1, results in increased cyclin D1 expression and decreased cyclin D3 expression.[16]

Notably, EWS/FLI1 increases expression of an oncogenic variant of cyclin D1, referred to as cyclin D1b, due to alteration of transcription mechanics from truncation of EWS in the EWS/FLI1 fusion protein. Wild type EWS is a member of the RNA- and DNA- binding TET family of proteins that is involved in transcriptional regulation and RNA splicing.[17] EWS binds and interacts with transcription and splicing machinery and favors D1a isoform expression, however the fusion protein EWS/FLI1, with a truncated transcriptional regulator EWS protein, favors D1b isoform expression, mediated through slowing of transcription elongation.[18,19]

EWS/FLI1 further influences cell cycle progression through other G1 regulatory genes. Antisense oligonucleotide mediated downregulation of EWS/FLI1 contributed to decreased expression of cyclin D1 and cyclin E, while expression of cyclin-dependent kinase inhibitors of the G1-S transition, p21 and p27, was increased. Transfection of EWS/FLI1 into NIH-3T3 cells resulted in the converse phenomenon.[20] Finally, loss of p16, a cyclin-dependent kinase inhibitor, is a frequent mutational event found in up to 30 percent of Ewing family of tumors and is associated with worse prognosis.[21] The multiple roles of EWS/FLI1 in activating mediators of G1 cycle progression, promoting cylin D1b expression and suppressing inhibitors of the G1-S transition, suggest that these pathways may be attractive therapeutic liabilities in Ewing sarcoma.

The role of NF-κB signaling in Ewing sarcoma

In addition to direct targets of EWS/FLI1 as mediators of Ewing oncogenesis, other signaling pathways have been identified that play an important role in Ewing sarcoma survival and growth.

The NF-κB pathway is known as a transcription factor involved in immune and inflammatory pathways. NF-κB is composed of five family members of proteins that are grouped

based on those that require proteolytic processing for activation and those that do not. RelA/p65, c-Rel and RelB proteins do not require proteolytic processing while NF-κB1 (p105) and NF-κB2 (p100) are processed to active forms p50 and p52, respectively. RelA/p65 and c-Rel proteins most frequently dimerize. Extrinsic, autocrine or instrinsic activation of the IKK complex can result in phosphorylation and proteolytic degradation of the NF-κB inhibitory protein, IκBα which binds to the nuclear localization sequence of NF-κB homo or hetero-dimers and blocks their nuclear localization.[22] In contrast, RelB, a NF-κB protein that is expressed mainly in lymphoid tissue dimerizes with NF-κB2 (p100) and requires proteolytic processing to allow for nuclear localization of the p52-RelB dimers.[22]

Dimers composed of RelA/p65, c-Rel and p50 are under the regulation of the canonical or non-canonical IKKs. Canonical IKKs include a complex of catalytic IKK proteins IKBKB and IKBKA as well as the regulatory subunit IKKγ/NEMO. In contrast, the non-canonical IKK proteins, IKBKE and TBK1 act independently to promote NF-κB activation[23,24], and play roles in cellular signaling involving activation of the anti-viral interferon response and Akt activation.[25]

The NF-κB family of proteins have been intensively studied for their role in inflammation and the innate immune response, in which NF-κB transcription factors express target genes involved in cell proliferation, survival and migration. Recent evidence suggests that aberrations in regulation of NF-κB signaling or chronic inflammation are associated with tumorigenesis.[22,26,27]

Numerous mechanisms underlie NF-κB mediated tumorigenesis but can include uncoupling of NF-κB transcription factors from the intricate and precisely controlled inhibitory regulators, autocrine or paracrine production of cytokines stimulating expression of NF-κB proteins as well as chronic infection and inflammation. Activation of NF-κB target genes results

in stimulation of cell proliferation through cytokine expression, expression of cyclin D1 and inhibition of apoptosis in response to genotoxic stress secondary to increased expression of cellular inhibitors of apoptosis (cIAPs) and BCL2 family member proteins. Increased angiogenesis and metastatic potential are also features of NF-κB transcriptional activation, mediated by expression of matrix metalloproteinases as well as angiogenic factors such as IL-8 and vascular endothelial growth factor (VEGF).[22]

In the cellular context of Ewing sarcoma, NF-κB signaling has been described to induce resistance to apoptotic stimuli.[28] Further, a role for NF-κB in mediating Ewing sarcoma turmorigenesis was suggested when expression of a degradation-resistant form of an inhibitor (IκBα) of NF-κB resulted in decreased tumorigenicity of Ewing sarcoma cells, with decreased ability to generate tumors in nude mice.[29]

Defining and targeting mediators of oncogenesis in EWS/FLI1 transformed cells

The central role of EWS/FLI1 in orchestrating expression of oncogenic mediators in Ewing sarcoma makes it an attractive therapeutic target; however, such therapies are difficult to develop. Transcription factors have remained poor targets for drug development due to the broad roles of transcription factors in normal tissue as well as tumor cells, and the challenges of designing therapeutic compounds that can localize to the nucleus. [30] Strategies to identify Ewing sarcoma specific tumor liabilities are necessary to develop improved targeted therapies. One such approach involved a large-scale screen of several hundred-cancer cell lines with 130 preclinical and clinical drugs to identify tissue-specific sensitivity and associations between cancer genes and cellular response. This screen resulted in the identification of marked sensitivity of Ewing sarcoma to PARP-inhibitors.[24] Further investigation of the mechanism underlying sensitivity of PARP inhibition extended our understanding of Ewing sarcoma biology, demonstrating that Ewing cells have greater foci of double strand breaks per cell even

when compared to other ETS mediated tumors, such as prostate cancer cell lines expressing *TMPRSS2-ERG*. [31,32]

To identify novel Ewing sarcoma tumor specific liabilities, we have conducted a near-whole genome functional shRNA screen of five EWS/FLI1 expressing Ewing sarcoma lines, compared to over 200 non-Ewing cancer cell lines. Candidate tumor specific liabilities were validated by shRNA knockdown and chemical inhibition *in vitro* and *in vivo*.

Materials and Methods:

shRNA screen and analysis

In collaboration with the Broad Institute and as a part of Project Achilles (http://www.broadinstitute.org/achilles)[33], a near whole genome pooled shRNA screen was performed in five EWS/FLI1 rearranged Ewing sarcoma cell lines (A673, EW8, EWS502, TC71 and TC32) and one EWS/ERG rearranged cell line (CADO-ES-1). The screen involved a total of 223 cell lines from 22 cancer types and was performed with an shRNA library of 55,541 barcoded shRNAs in lentiviral vectors targeting 13,882 genes.[33] Cells were infected at a multiplicity of infection of 0.1 and cultured following infection for at least 16 doublings. DNA from cells was then collected and sequenced to quantify the abundance of each shRNA, with depleted shRNAs hypothesized as targeting essential genes. Quality control tests were applied to remove replicates that failed quality control measures, along with overlapping shRNAs and shRNAs with low counts in DNA samples. All Ewing cell lines, except TC32, and 211 other tumor lines passed the quality control tests. Filtered quality controlled data were presented as ZMAD scores genome-wide normalized per individual cell line.

In order to prioritize targets that are uniquely essential for the proliferation and survival of Ewing sarcoma cell lines, we tested the differential expression of the shRNAs in Ewing versus other cancer cell lines that display low functional similarity with Ewing sarcoma. Functional non-similarity with Ewing sarcoma was estimated based on a consensus of published EWS/FLI1 gene signatures[13,34,35] and principle components analysis applied on Achilles matched gene expression data.

To determine whether a given shRNA contributes to the observed essentiality phenotype between Ewing and non-similar Ewing classes, we used a weight of evidence (WoE) approach. This approach computes the likelihood that a given shRNA has the ability discriminate between

the two classes of interest in a statistically significant manner. Weights of evidence scores for a particular class comparison, as defined by a class definition file, were calculated using the GenePattern module "ScorebyClassComp."[36]

The RIGER module implemented in the GENE-E program (http://www.broadinstitute.org/cancer/software/GENE-E), was used to collapse shRNA differential essentiality scores to gene rankings by the weighted sum of the best two hairpins method.[37] The top gene hits identified based on the RIGER method were then filtered out for expression based on the z-score threshold of 1.0 in the RNASeq Ewing sarcoma cell line and tumor data available through the SIGMA Project (Stegmaier Lab).

Cell lines and chemical compounds

A673, EW8, SKNEP, EWS834 and RDES cells were grown in Dulbecco's Modified Eagle's Media (Life Technologies) supplemented with 10% fetal bovine serum (FBS, Sigma-Aldrich) and 10 units/mL of penicillin, 10 μg/mL streptomycin and 30 μg/mL of L-Glutamine, (PSQ, Thermo Fisher Scientific). A673 cells were cultured in media supplemented with 1 mmol/L of sodium pyruvate (Life Technologies). CADO-ES-1, TTC466 and EWS502 cell lines were cultured in RPMI 1640 media (Life Technologies) supplemented with 15% FBS and PSQ. TC71 and TC32 lines were cultured in 10% RPMI1640 and PSQ media.

Cell lines were kindly provided by Dr. Todd Golub (Broad Institute, Cambridge, MA) except for EWS502 and EWS834, which were gifts from Dr. Jonathan Fletcher (Brigham and Women's Hospital, Boston, MA). All cell lines have been confirmed to have an EWS/FLI1 or EWS/ERG rearrangement by RNA sequencing. All cell lines were cultured at 37°C in a humidified atmosphere containing 5% CO_2. Chemical compounds utilized included the JAK1/2 and IKBKE/TBK1 inhibitor CYT387 (Selleck Chemicals), an IKBKE/TBK1 inhibitor MRT67307, kindly gifted by Dr. David Barbie (Dana-Farber Cancer Institute, Boston, MA), a

sesquiterpine lactone inhibitor of IKBKB, parthenolide (Selleck Chemicals), a JAK 1/2 inhibitor, Ruxolitinib (Selleck Chemicals), Akt inhibitor MK-2206 (Selleck Chemicals) and the PI-3K inhibitor GDC-0941 (Selleck Chemicals). Ewing sarcoma cell lines were also treated with the CDK4/6 inhibitor LEE011, gifted to us from Novartis Oncology (Cambridge, MA), and PD-0332991 (Selleck Chemicals). Compounds were dissolved in DMSO and stored at 10 mmol/L stock concentrations at -20°C for up to several months for *in vitro* experiments. For *in vitro* drug treatments, Ewing sarcoma cell lines were plated in 6-well or 10 cm tissue culture plates, allowed to adhere over 24 hours and subsequently treated with the above listed compounds.

Determination of cell viability and colony formation

Cell viability was assessed using the CellTiter-Glo Luminescent Cell Viability Assay (Promega) that measures ATP content as a surrogate for cell number. Luminescent readings were obtained using the FLUOstar Omega microplate reader (BMG Labtech). For small-molecule treatments, cells were seeded at a density of 1.25 $x10^3$ cells per well in a 384-well plate (Corning). Cells were treated at a range of concentrations and IC_{50} values were calculated from ATP luminescence measurements after five days of treatment using log-transformed, normalized data in GraphPad Prism 5.0 (GraphPad Software, Inc.). Cell viability was also determined following shRNA-tranduction of Ewing sarcoma cells. After seeding 1.25$x10^3$ cells per well in a 384-well plate, ATP content was measured at day 3, 5, 6 and 8 after transduction.

Colony formation assays were performed by dissolving 5 $x10^3$ cells into 2 mL of methylcellulose matrix (ClonaCell-TCS Medium, Stemcell Technologies) and subsequently plating them into gridded 6-cm plates (Thermo Fisher Scientific) and incubated for 10 to 15 days. Colonies were counted from 100 squares using a Nikon inverted microscope. All samples were plated in duplicate.

Cell Cycle analysis and Apoptosis

The effect of small-molecule treatment on Ewing sarcoma cell cycling was measured at 72 and 120 hours post-treatment. Cells were harvested, washed in PBS, suspended in 200 μL of PBS and fixed with 4 mL of cold 70% ethanol added drop-wise. Tubes were stored at -20°C for up to one week prior to analysis. Tubes were centrifuged at 500g for 10 minutes and washed with PBS before being re-suspended in 200-500 μL of staining buffer containing 40 μg/mL of propidium iodide (Sigma Aldrich) and 100 μg/mL of RNase A (Qiagen). Samples were incubated in the dark for at least fifteen minutes before analysis on a FACSCanto II analyzer. Data analysis was completed using Flowjo 7.6 Software (Treestar, Ashland OR, USA).

Ewing sarcoma cells lines were assessed for apoptosis after small-molecule treatment for 72 hours to up to 120 hours post-treatment. Apoptosis was assessed using flow cytometric analysis of annexin V and propidium iodide staining (eBioscience). Following drug treatment, cells were harvested, washed with phosphate-buffered saline (PBS) and annexin binding buffer (eBioscience) before incubation with annexin V-APC, washed with annexin binding buffer and stained with propidium iodide.

Western blotting

Protein Extraction: Whole cell lysates were prepared following small-molecule treatment or six days after shRNA transduction. Cells were washed with PBS, trypsinized and lysed using 1x Cell Lysis Buffer (Cell Signaling) supplemented with EDTA-free protease inhibitors (Complete Mini) and PhosSTOP phosphatase inhibitors (Roche). Lysates were incubated with cell lysis buffer for fifteen minutes and centrifuged at 13,000 rpm for fifteen minutes at 4°C. Supernatants were removed and evaluated for protein concentration using the Bradford method (Bio-Rad Protein Assay Dye Reagent Concentrate).

Nuclear extraction: Nuclear extracts were prepared using a nuclear extraction kit from ActivMotif. Ewing sarcoma cells, grown in a 10-cm tissue culture plate, were washed with ice-

cold PBS containing phosphatase inhibitors and harvested with a cell-scraper in 3 mL of PBS with phosphatase inhibitors. Cells were spun down at 500 rpm for five minutes and incubated on ice for ten minutes with a hyptonic buffer. The cell membrane was then disrupted with addition of detergent and gentle agitation. The cytoplasmic subfraction was separated with centrifugation at 13,000 rpm for one minute and aspirated away from the nuclear pellet. The nuclear pellet was washed with hypotonic buffer before being resuspended in complete lysis buffer containing protease inhibitors and DTT. Following thirty minutes of incubation on ice with complete lysis buffer, nuclear protein was separated from the remaining sub-cellular pellet with centrifugation at 13,000 rpm for ten minutes. Supernatants were removed and evaluated for protein concentration using the Bradford method (Bio-Rad Protein Assay Dye Reagent Concentrate).

Immunoblotting: Lysate concentrations were standardized and resolved on 4-12% Nu-PAGE Bis-Tris gels (Life Technologies) and electrophoretically transferred to Immobilon-P PVDF membrane (Millipore) activated in methanol. Membranes were blocked in 5% bovine serum albumin (BSA) diluted in TBS-tween and hybridized using primary antibodies diluted in 5% BSA TBS-Tween and 0.1% sodium azide.

Antibodies utilized: Primary antibodies utilized included PARP-1 (Cell Signaling), GAPDH (Santa Cruz), Vinculin (Abcam), IKBKE (Sigma Aldrich), TBK1 (Cell Signaling), IκBα (Cell Signaling), NF-κB p65 (Cell Signaling), NF-κB p50 (Santa Cruz), NF-κB p52 (Santa Cruz), c-Rel (Cell Signaling), Rel B (Cell Signaling), CDK4 (Thermo Fisher Scientific), CDK6 (Cell Signaling), CCND1 (EMD Millipore), STAT3 (Cell Signaling), pSTAT3 Y705 (Cell Signaling), pTBK1 S172 (Cell Signaling), Akt (Cell Signaling), pAkt T308 (Cell Signaling), pAkt S473 (Cell Signaling), pRb S780 (Cell Signaling), pRb S795 (Cell Signaling), and Rb (Cell Signaling). Following overnight incubation at 4°C with primary antibody, membranes were washed with TBS-Tween and hybridized with mouse and rabbit horseradish peroxidase (HRP)-

conjugated secondary antibodies (1:5000, GE Healthcare) diluted in TBS-Tween. Protein-antibody complexes were detected by enhanced chemiluminescence with Amersham ECL Prime reagent (GE Healthcare).

Establishment of tumor xenografts in NSG mice

CYT387 treatment

Mouse studies were conducted using Institutional Animal Care and Use Committee (IACUC) approved animal protocols in accordance with institutional guidelines at the Lurie Family Imaging Center. Tumor xenografts were established using TC32 cells. Approximately 5 $x10^6$ cells were suspended in 30% matrigel and subcutaneously injected into 6-week old female NSG mice (Jackson Laboratories). Treatments began when tumor volume reached 100-250 mm^3. Nine mice were treated with CYT387 at 100 mg/kg daily and ten mice with vehicle. CYT387 was dissolved in N-methyl-2-pyrrolidone (NMP) at a concentration of 1 mg CYT/10 uL NMP and dissolved in a 1:10 ratio in methylcellulose/tween (0.5%) and 0.4% polysorbate-80 in sterile water. Treatments were administered by oral gavage, once daily, seven days a week over the course of 28 days. Tumor volumes were measured with calipers and animals were sacrificed when tumor volumes exceeded 2,000 mm^3. Tumor xenografts were preserved by flash freezing as well as formalin fixation for further analysis.

LEE011 treatment

Tumor xenografts were established in forty-five NSG mice using $5x10^6$ TC32 cells resuspended in 30% matrigel and injected into the flank. Treatments began when tumor volume reached 100-250 mm^3. LEE011 was resuspended in 0.5% carboxymethylcellulose and delivered at doses of 75 mg/kg or 250 mg/kg by oral gavage seven days a week for 21 days. Thirteen mice were in the vehicle, 75 mg/kg and 250 mg/kg cohort and three mice per cohort were sacrificed to evaluate the pharmacodynamics of the compound following the fifth dose. Tumor volumes were

measured with calipers and animals were sacrificed when tumor volumes exceeded 2,000 mm^3. Tumor xenografts were flash frozen or formalin fixed for further immunohistochemical staining.

Results:

IKBKE scores highly in a near whole genome shRNA screen of Ewing sarcoma

IKBKE is a member of the non-canonical IKK family, along with the closely homologous protein TBK1, and is an important regulator of innate immune activity through activation of interferon α and β. Both IKBKE and TBK1 have also been shown to affect NF-κB signaling and to play a role in cancer cell survival and tumorigenesis.[26,27,38] *IKBKE* is a putative oncogene in breast cancer, with approximately one-third of primary breast cancer samples showing copy-number gain of this gene, and amplification of *IKBKE* is observed in 16.3% of breast cancer cell lines.[27] In addition to promoting activation of NF-κB, IKBKE and TBK1 have been shown to directly phosphorylate Akt.[23,24] There is also evidence to suggest that IKBKE may be important in the cellular response to DNA damage or in the mediating stress response associated with oncogene expression through activation of NF-κB.[39,40]

IKBKE was one of the top one hundred hits in the near whole-genome, pooled shRNA screen for essential gene liabilities in four EWS/FLI1 expressing Ewing cell lines (Supplemental Table 1). Targeting of IKBKE with shRNA led to the preferential depletion of Ewing sarcoma cells, as compared to 83 non-similar cancer cell lines. Non-similar cancer cell lines, among those tested in Project Achilles, were defined based on lack of gene expression similarity to a consensus of published EWS/FLI1 gene signatures[13,34,35] and principle components analysis applied on matched gene expression data. In addition to IKBKE, other NF-κB pathway proteins, including the canonical IKK, IKBKB and NF-κB1 also scored as top hits in the shRNA screen (Figure 1A, B).

We noted that IKBKE protein is expressed as a doublet at levels similar to that expressed in MCF-7 breast cancer cells that are dependent on IKBKE (Figure 1C). We then validated the dependence of Ewing cell lines on IKBKE through shRNA mediated knockdown of IKBKE

using the second best hairpin from the whole genome shRNA screen as well as two additional shRNA sequences, all of which do not target TBK1 or other canonical IKK proteins (Supplemental Table 2). Knockdown of IKBKE resulted in impaired viability and decreased colony formation across four Ewing sarcoma cell lines (Figure 2). We saw a similar dependence of Ewing sarcoma cell lines on the highly-homologous non-canonical IKK protein, TBK1 (Supplemental Figure 1). TBK1 and IKBKE have similar cellular functions, and dependence on both IKBKE and TBK1 has been demonstrated in the context of breast cancer cells, such as MCF-7, in which shRNA mediated knockdown of these genes showed that the cell line required both genes for proliferation.[27]

Chemical inhibition of IKBKE results in impaired viability and colony formation of Ewing sarcoma cells

In addition to evaluating the effect of downregulation of total IKBKE protein, as is the case with shRNAs, we also investigated the effects of small-molecule inhibition of the kinase activity of IKBKE on Ewing sarcoma cell growth and colony formation.

Ewing sarcoma cell lines were treated with MRT67307, a novel inhibitor of IKBKE/TBK1 and CYT387 a JAK 1/2 inhibitor with activity against IKBKE/TBK1.[25,41-43] Both of these inhibitors act at the highly conserved kinase domain of the non-canonical IKKs and competitively inhibit phosphorylation, with on-target activity of IKBKE/TBK1 inhibition marked by paradoxical increases in phosphorylation at Serine-172 on TBK1.[25]

We tested the effects of CYT387 and MRT67307 on cell growth and anchorage independent growth in a panel of ten Ewing sarcoma cell lines. Cells were treated for five days with CYT387 and MRT67307 at a range of concentrations using 2-fold serial dilutions. Treatment with CYT387 impaired cell viability in all cell lines, with an average IC_{50} of 3.95 μM (range: 2.07-6.65 μM) (Figure 3B). Similarly, MRT67307 impaired cell viability in all cell lines

with an average IC_{50} of 1.67 μM, ranging between 0.24 μM to 5.66 μM (Figure 3A). There was a high degree of similarity between the pattern of sensitive and non-sensitive cell lines to MRT67307 and CYT387 (Figure 3A). Ewing cell lines were also treated with Ruxolitinib, a JAK 1/2 inhibitor, as a control for the effect of inhibition of this pathway on Ewing sarcoma cell viability. Ruxolitinib did not inhibit cell viability, with the exception of TC32 and EWS502, which had calculated IC_{50}'s of 15.71 μM, and 33.36 μM, respectively (Figure 3C), suggesting that the effects of CYT387 on Ewing sarcoma cell viability and anchorage independent growth are unlikely to be related to downregulation of JAK signaling.

We subsequently tested the role of CYT387 to impair colony formation in a methylcellulose matrix with continuous exposure to CYT387 over a range of doses from 0 to 10 μM. Anchorage independent growth was reduced with CYT387 in a concentration dependent manner, corresponding to the IC_{50} of each cell line, with the exception of EWS502, which had greater sensitivity to CYT387 as, measured by colony formation than impairment of cell viability (Figure 3D).

On target activity of CYT387 and MRT67307 was assessed with evaluation of p-TBK1 (S172) levels after treatment of TC32 cells over a time course of 1, 6 and 24 hours. Paradoxical elevation of p-TBK1 (S172) is a marker for inhibition of IKBKE and TBK1. p-TBK1 (S172) was elevated after one hour of treatment with MRT67307 and CYT387 but not with Ruxolitinib treatment (Figure 3E). CYT387 also inhibited JAK 1/2 and resulted in a decrease in p-STAT3 (Y705), as did Ruxolitinib. The decrease in p-STAT3 levels was noted as early as one hour with Ruxolitinib treatment but only after twenty-four hours with CYT387 treatment (Figure 3E).

We then chose to investigate the role of pharmacologic IKBKE/TBK1 inhibition on downstream cellular signaling pathways. Notably, both IKBKE and TBK1 have been shown to be oncogenic kinases that promote tumor survival and proliferation through activation of the NF-

κB pathway. While canonical IKK proteins, such as IKKß, IKKγ and IKKα, have long been known to promote NF-κB activation through phosphorylation and downstream ubiquitin-mediated degradation of the NF-κB inhibitor, IκBα, recent evidence suggests that the non-canonical IKKs also function in this pathway. In addition to the role of IKBKE and TBK1 in innate immunity through IRF-mediated activation of the interferon antiviral response, these non-canonical IKKs phosphorylate and target IκBα for degradation.[38] Additionally, both TBK1 and IKBKE directly phosphorylate and promote nuclear localization of the NF-κB family protein c-Rel, independently of IKBKB signaling.[44] Following six hours of treatment with CYT387 and thirty minutes of stimulation with 30 ng/mL of TNF-α, we noted impaired degradation of IκBα as compared with DMSO treated controls in TC32 and HEK-293T cells (Figure 3G). Following forty-five minutes of TNF-α stimulation, there was impaired nuclear translocation of NF-κB family proteins c-Rel and RelA/p65 in the setting of CYT387 treatment as compared with DMSO treated controls in both cell lines (Figure 3G). The effect of CYT387, which acts on IKBKE/TBK1, on impairing NF-κB activation was similar to the effect of parthenolide, an inhibitor of the canonical NF-κB pathway. However, we also noted mildly impaired nuclear translocation of NF-κB p50 in samples treated with CYT387, which was not seen in parthenolide, or DMSO treated samples (Figure 3G).

Additionally, IKBKE and TBK1 have been reported to directly promote Akt phosphorylation at serine-473 (S473) and threonine-308 (T308), independent of PI-3K, PDK1 and mTORC2 [23,24]. Thus, we evaluated the impact of chemical inhibition with CYT387 and MRT67307 on Akt phosphorylation. In contrast to the PI-3K inhibitor, GDC-0941, and an Akt inhibitor, MK-2206, we did not observe any effect on p-Akt S473 phosphorylation at six or twenty-four hours following treatment with 5 uM of MRT-67307 or CYT387. There was a

transient decrease in phosphorylation of the T308 site following six hours of treatment with CYT387, MRT-67307 and greater inhibition of T308 phosphorylation with GDC-0941 and MK-2206, however, this effect was not sustained for the twenty-four hour treatment period with either the IKBKE/TBK1 inhibitors or the PI-3K pathway inhibitors (Figure 3F).

We also noted cytotoxic effects of IKBKE/TBK1 inhibition with CYT387 and MRT67307, which resulted in the elevation of cleaved PARP-1 and dsDNA breaks as assessed with elevation in phosphorylated H2A.X following twenty-four hours of treatment (Figure 3F). IKBKE has previously been shown to protect against DNA-damage induced cell death, through nuclear localization, DNA-damage dependent SUMOylation and subsequent phosphorylation of the NF-κB p65 substrate that promotes expression of anti-apoptotic genes.[40] An impairment of IKBKE may further exacerbate apoptosis in response to DNA damage in a cellular context, such as Ewing, that has been shown to be more sensitive than other tumor types to DNA-damaging agents such as camptothecin, cisplatin and mitomycin-C as well as to PARP-1 inhibition.[31,32]

IKBKE/TBK1 inhibition in Ewing sarcoma cells results in increased apoptosis but not significant G1 cell cycle arrest

We evaluated the mechanism for impairment of cell viability in Ewing sarcoma cells following inhibition of IKBKE/TBK1 with CYT387 or MRT67307. We treated two highly sensitive Ewing cell lines, SKNEP and TC32, and a relatively less sensitive Ewing line, TC71 with 5 μM of CYT387 for 24 and 72 hours and measured apoptosis with Annexin V/propidium iodide staining. Apoptosis was consistently elevated more than two times control at 72 hours after treatment of the SKNEP, TC32 and TC71 cell lines (Figure 4A).

Next, we evaluated the role of CYT387 and MRT67307 on cell cycle progression with a particular eye towards the impact of CYT387 on cell cycle arrest. KINOMEscan assay analysis

of CYT387 had been performed in an acellular context. This competitive binding assay involves a kinase-tagged phage, test compound and an immobilized ligand to which the kinase is bound. Binding of compound to kinase displaces the kinase from the immobilized ligand. The amount of kinase bound to immobilized ligand is determined and represented as a percent of DMSO with higher values representing decreased interaction between kinase and compound. In this assay, interaction of CYT387 and CDK4 was noted, however with less affinity than that between CYT387 and IKBKE.[45] *In vitro* treatment of four Ewing cells with CYT387 did result in decreased p-Rb S780, a marker of CDK4 inhibition, following one hour of treatment. However, this was not noted with MRT67307 (Figure 4B).

Thus, we also wanted to test the impact of CYT387 on cell cycle arrest, in comparison to MRT67307 and LEE011, a highly specific CDK 4/6 inhibitor. We chose one cell line (TC32) with high sensitivity to CYT387 and MRT67307 and one cell line (TC71) with relatively decreased sensitivity to these compounds. In comparison to treatment with LEE011 where G1 arrest is observed, we did not observe G1 arrest with these two compounds. Rather, an increase in G2 phase was noted with increasing doses of CYT387 and MRT67307 (Figure 4C).

CYT387 treatment in vivo results in significantly decreased tumor size and prolonged survival in a Ewing sarcoma cell line xenograft

To evaluate the role of IKBKE *in vivo*, we tested the inhibition of IKBKE/TBK1 with CYT387 and demonstrated that CYT387 significantly inhibited tumor xenograft growth of established tumors at fifteen days after treatment (p-value = 0.036) and improved survival as compared to vehicle control, (p-value = 0.0231) over the course of twenty-nine days of treatment (Figure 5A). Mice did not experience any weight loss or other apparent side effects over the course of treatment with CYT387 (Figure 5B). Tumor xenografts were frozen and evaluated for changes in p-TBK1 (S172) by immunoblotting. Two vehicle treated mice which were sacrificed

when tumor volume exceeded 2000 mm^3 on day 16 and 20 and two CYT387 treated mice which were sacrificed at day 20 and day 27 were selected for analysis and showed marginal elevation of the p-TBK1 S172 mark in the CYT387 treated groups (Figure 5C).

G1 cell cycle proteins (CDK4, CCND1) score highly in a near whole genome shRNA screen

G1 cell cycle proteins CDK4 and cyclin D1 (CCND1) also scored among the top ten percent of hits in the near whole genome shRNA screen of Ewing cell lines. Targeting of CDK4 and CCND1, but not CDK6, with shRNAs resulted in preferential depletion of Ewing sarcoma cell lines as compared to non-similar cancer cell lines (Figure 6A).

Cyclin D1 is among the most frequently amplified genes in many cancers and the overexpression of cyclin D1 has been associated with shortening of the G1 interval.[46] Ewing sarcoma dependency on cyclin D1 and CDK4 is supported by elevated mRNA expression of CCND1 and CDK4 in Ewing sarcoma cell lines as compared with cell lines from other tumor types (Figure 6D). RNAseq analysis of the Ewing sarcoma cell lines confirms elevation in cyclin D1 and CDK4 mRNA levels and is reflective of cyclin D1 and CDK4 expression among a panel of twenty-two patient tumors (Figure 6C). Notably, CDK6, which also interacts with cyclin D1 in regulation of the G1 phase, is poorly expressed across all Ewing sarcoma cell lines and primary tumor tissue and did not score within our near-whole genome shRNA screen.

Additionally, there is evidence to suggest that EWS/FLI1 may engender sensitivity to cell cycle inhibition. A large scale screen across 700 cancer lines with the CDK 4/6 inhibitor, PD-0332991, demonstrated that expression of EWS/FLI1 was a significant marker of increased drug sensitivity (p-value = 0.033, calculated by the Mann-Whitney test) (Figure 6B).[47]

To validate the findings of the near-whole genome shRNA screen in Ewing sarcoma cell lines, we performed shRNA knockdown of CDK4 and cyclin D1 in two Ewing sarcoma cell lines, TC32 and TC71. Knockdown of CDK4 and cyclin D1 resulted in impaired anchorage

independent growth and cell viability. Further, we noted a pattern of increased sensitivity among TC32 cells for CDK4 and cyclin D1 inhibition as compared with TC71, which was subsequently recapitulated in patterns of sensitivity to pharmacologic inhibition of CDK4 (Figure 7).

Pharmacologic inhibition with LEE011, a specific CDK4/6 inhibitor, induces G1 arrest with apoptosis in a subset of cell lines

Following validation of decreased cell viability and impaired anchorage independent growth of Ewing sarcoma cell lines in the context of shRNA mediated knockdown of CDK4 and cyclin D1, we chose to evaluate the effect of pharmacologic inhibition of CDK4 on Ewing sarcoma viability and cell cycle phase with LEE011 (Novartis Oncology), a specific dual CDK4/6 kinase inhibitor. We cultured a panel of ten Ewing sarcoma cell lines with a range of two-fold serially diluted doses and measured cell viability following five days of treatment. The average IC_{50} across cell lines was 6.48 μM with a range of 0.26 -18.06 μM. There was a group of highly sensitive cell lines (TC32, SKNEP, EWS384), with sensitivity at sub-micromolar concentrations of LEE011 (Figure 8A, B). Next we evaluated the impact of LEE011 on cell cycle phase over a logarithmic concentration curve including concentrations of 0.1 μM, 1 μM and 10 μM. G1 arrest was noted in a concentration-dependent fashion with more sensitive cell lines arresting at 1 μM or less. The least sensitive cell lines, EW8 and TC71, showed only a moderate elevation in the G1 phase following five days of treatment with 10 μM of LEE011 (Figure 8C). In addition to G1 arrest there is also induction of apoptosis in a subset of cell lines highly sensitive to LEE011. Treatment of TC32, SKNEP, EWS834 and RDES with 1 μM of LEE011 results in more than a three-fold increase in annexin V staining cells while treatment of the least sensitive cell lines, EW8 and TC71, results in little to no induction of apoptosis (Figure 8D). Finally, we demonstrated in a panel of both relatively sensitive (TC32 and SKNEP) and

relatively resistant (TC71 and EW8) cell lines that LEE011 treatment was on-target, resulting in decreased pRb-S780, a downstream target of CDK4 activity (Figure 8E).

Effect of in vivo treatment with LEE011

Following *in vitro* validation of cyclin D1 and CDK4 through small-molecule inhibition and shRNA-mediated knockdown, we assessed the efficacy of LEE011 *in vivo* using a mouse xenograft model of Ewing sarcoma. NSG mice injected with subcutaneous xenografts were treated with vehicle, 75 mg/kg or 250 mg/kg of LEE011 by daily oral gavage. Toxicity was noted at the highest treated dose of 250 mg/kg with one mouse being found dead on day five. An additional two mice were noted to be in distress and were sacrificed at ten and twelve days following treatment. On necropsy, these mice were noted to have bloated abdomens with the intestines and stomach being distended with air, suggestive of a clinical ileus. Mice in the 75 mg/kg/day group had a mild initial decrease in weight to a nadir of 93% baseline but returned to near baseline after receiving a drug holiday and supplemental nutrition and hydration (Figure 7B, C). Mice in the 250 mg/kg/day group had a mild but significant weight loss to a nadir of 94% of their baseline weight.

Treatment with LEE011 resulted in marked attenuation of tumor growth at both the 75 mg/kg ($p < 0.001$) and 250 mg/kg dose ($p < 0.001$) and partial tumor regression was noted at the highest treatment dose following fifteen days of treatment (Figure 7A). Although toxicities were noted in the high dose group at 250 mg/kg, the 75 mg/kg dose is also effective at attenuating tumor growth and closely estimates the clinically relevant dose of 400 – 600 mg/day being utilized in clinical trials of LEE011.

Evaluating mechanisms of sensitivity to LEE011

Within our panel of Ewing sarcoma cell lines there is a range of sensitivity to LEE011 from sub-micromolar to low micromolar doses. We sought to identify markers of sensitivity to

inhibition of CDK4 and evaluated the expression or mutation of several related and regulatory proteins. Low expression of p16 (CDKN2A), an inhibitor of the G1 phase cyclins, and high expression of Rb, a tumor suppressor that is the target of CDK4/6 phosphorylation, have been reported to predict sensitivity to CDK 4/6 inhibition.[48] We tested this hypothesis by evaluating the expression of Rb and p16, assessed by RNAseq, in three highly sensitive (IC_{50} <1 uM at five days of treatment) Ewing sarcoma lines as compared to the remaining lines. We noted that p16 expression was uniformly low and did not significantly vary between the two cohorts (p-value: 0.634). While Rb expression by RNAseq was significantly (p-value: 0.044) lower in the cohort of cell lines with decreased response to LEE011, there was a great deal of variability in Rb expression in the three highly sensitive cell lines. Further, endogenous p-Rb levels were similar in the most sensitive and least sensitive Ewing sarcoma lines (Figure 8E).

We next evaluated whether known mutations in the Ewing sarcoma cell lines are associated with sensitivity to LEE011 treatment. EWS/FLI1 fusion type was not associated with response. Furthermore, the majority of Ewing sarcoma cell lines had loss of p16 and the adjacent tumor suppressor p15INK4b (CDKN2B), which binds CDK4/6 and prevents activation by cyclinD. These features were also not predictive of sensitivity. Similarly, *TP53* was also mutated in the majority of Ewing sarcoma cell lines (Figure 10 A).

Recently, it has been reported that Cyclin D1b, an oncogenic splice variant of cyclin D1, is upregulated in several cancers, and its expression associated with increased invasiveness and poorer disease outcomes.[49] The aberrant splicing of cyclin D1b results in the loss of regulatory regions that influence protein turnover and sub-cellular localization, enhancing its transformative potential and nuclear localization. Additionally, the EWS/FLI1 protein has been shown to increase cyclin D1b expression through alterations in the dynamics of transcript elongation.[18,19] We observed variable levels of cyclin D1b mRNA expression as compared to cyclin D1a in a

panel of Ewing sarcoma lines. Interestingly, decreased ratios of cyclin D1b/cyclin D1a mRNA were noted in cell lines (RDES, TC32, and SKNEP) that have increased sensitivity to LEE011, suggesting that cyclin D1b expression may engender resistance to treatment with LEE011 (Figure 10C). We plan to further test this hypothesis by inducing expression of cyclin D1b in cell lines highly sensitive to LEE011 and evaluating the effect on the dose of the small molecule required to induce G1 arrest, apoptosis and decreases cell viability.

Discussion:

Ewing sarcoma is a pediatric tumor that despite advances in outcome for patients with localized disease continues to have poor outcomes for patients with relapsed or metastatic disease.[1,2] As is the case for other pediatric tumors with defining abnormalities of transcription factors, Ewing sarcomas have low mutation rates. The tumor driver event is the formation of the EWS/FLI1 fusion protein that results in the activation of an aberrant transcriptional program involving induction of oncogenes[12,13,15,50,51] and repression of tumor suppressor and mesenchymal fate genes.[34,50,52]

Integrative functional genomics approaches, involving genome scale RNAi screens, combined with evaluation of gene expression and genomic alterations, can provide insights into the biology of Ewing sarcoma. We applied such an approach to Ewing sarcoma to identify novel vulnerabilities that are preferentially depleted in EWS/FLI1 expressing cells compared to non-Ewing sarcoma cancer cells. We have identified novel therapeutic targets and demonstrated the importance of non-canonical IKK signaling and G1 cell cycle regulation as mediators of Ewing sarcoma cell survival.

IKBKE is a regulator of innate immunity and an oncogenic kinase

IKBKE, along with the highly homologous non-canonical IKK, TBK1, have classically been demonstrated to be involved in innate immune responses to viruses through activation of interferon expression. Both IKBKE and TBK1 are capable of binding to and assembling with TRAF3 and TANK to phosphorylate serine and threonine residues on interferon regulatory factors 3 and 7 which results in nuclear translocation and production of IFN-α/β.[25,38,53]

The non-canonical IKKs, IKBKE and TBK1, can also regulate activation of the NF-κB family of proteins, in addition to canonical catalytic IKKs such as IKKα and IKKβ. Like the canonical IKK proteins, IKBKE and TBK1 phosphorylate and promote proteasome-mediated

destruction of IκBα. However, in contrast to the canonical IKK protein IKBKB, which phosphorylates two sites (Ser-32 and Ser-36) on IκBα, IKBKE binds to and phosphorylates only Ser-36 residue of IκBα while TBK1 uniquely targets only Ser-32 of IκBα.[38] While phosphorylation at a single residue with IKBKE has been shown to induce turnover of IκBα[27,54], it is possible that IKBKE and TBK1 activity on mediating IκBα destruction is complementary, with inhibition of both proteins resulting in greater efficiency of IκBα stabilization.

IKBKE affects other components of the NF-κB signaling pathways. Exogenous expression of IKBKE induces RelA/p65 phosphorylation at Ser-536 and accordingly, mouse embryonic fibroblasts (MEFs) deficient in IKBKE showed decreased phosphorylation at this site.[53] However, upon cytokine stimulation, phosphorylation is not entirely lost at this site in MEFs deficient in the non-canonical IKKs, suggesting that the canonical IKKs are sufficient to maintain phosphorylation at this site.[53]

In addition to phosphorylation and activation of the transactivation domain of RelA/p65, IKBKE directly activates NF-κB family protein, c-Rel and induces nuclear translocation. Both TBK1 and IKBKE directly phosphorylate the C-terminal domain of c-Rel, which results in dissociation of c-Rel from IκBα, independently of IKKβ signaling.[44]

IKBKE has also been shown to peturb NF-κB phosphorylation within the nucleus. IKBKE expression protects against DNA-damage induced cell death through nuclear localization following genotoxic stress. IKBKE is then SUMOylated at a lys-231 residue and subsequently triggers phosphorylation of nuclear p65, mediating the expression of anti-apoptotic proteins in response to DNA damage.[40]

Recent evidence has shown IKBKE to be an oncogenic kinase, with its transformative and tumorigenic activity mediated through NF-κB pathway signaling. Aldi et. al. first observed that IKBKE expression was elevated in a number of cancer cells lines including prostate, breast

and cervical cancer lines. Expression of IKBKE in these cell lines correlated with elevated phosphorylation at Ser-536 of p65, while elevation of the catalytic canonical IKKs was not correlated, suggesting that IKBKE promoted NF-κB activation.[53] More recently, integrative genomics approaches have demonstrated that *IKBKE* is a human breast cancer oncogene, amplified and overexpressed in a significant percentage of breast cancer cell lines and primary tumor specimens. IKBKE was also shown to lead to cell transformation upon overexpression in immortalized human cell lines and loss of IKBKE in human breast cancer cell lines resulted in impaired viability. The mechanism of IKBKE mediated transformation was suggested to be through activation of NF-κB. ShRNA mediated downregulation of IKBKE in breast cancer cell lines resulted in suppression of NF-κB target genes, and conversely, overexpression of IKBKE in human breast epithelial cells resulted in induction of an NF-κB transcriptional profile. Furthermore, IKBKE overexpression resulted in cytoplasmic degradation of IκBα and primary breast cancer specimens showed elevated nuclear localization of c-Rel that was significantly associated with the level of IKBKE expression.[27]

Additional research has demonstrated that IKBKE promotes NF-κB activation through multiple effectors. Hutti et. al. utilized an unbiased proteomic approach, involving a positional scanning peptide library to identify direct IKBKE substrates involved in mediating cell transformation.[55] This screen identified serine-418 of tumor suppressor CYLD as a direct target of IKBKE phosphorylation. Phosphorylation at this site resulted in decreased deubiquitinase activity of this protein and facilitated transformation of NIH-3T3 cells. A mutant form of CYLD S418A, with an absent IKBKE phoshorylation site, was capable of inhibiting IKBKE mediated NF-κB activation in MCF-7 cells. Inhibition of CYLD by IKBKE is relevant and necessary for IKBKE mediated cellular transformation. CYLD downstream targets for Lys63 linked de-ubiquitination include inflammatory mediators such as TRAF2, TRAF6 and NEMO.

Deubiquitination destabilizes these substrates and inhibits NF- κB mediated inflammatory signaling.[55]

Tumor necrosis factor receptor-associated factor 2 (TRAF2), in particular has been shown to be an important mediator of NF-κB signaling and is ubiquitinated following TNF-α stimulation. Subsequent work has shown that, TRAF2 is an effector of IKBKE transformation in mammary epithelial cells and that IKBKE directly phosphorylates TRAF2, promoting subsequent Lys63 mediated ubiquitination and NF-κB activation.[56,57]

IKBKE is an essential and targetable kinase in Ewing sarcoma

IKBKE, a member of the non-canonical IKK family, is an oncogenic kinase that has overlapping functions with the highly homologus protein TBK1. As discussed above, there is ample evidence demonstrating that the non-canonical IKKs act on several regulatory proteins, and integrate numerous pathways to promote tumorigenesis through NF-κB activation.

Here we used functional genomics approaches to identify IKBKE, a known breast cancer oncogene, as an essential kinase in Ewing sarcoma. Subsequently, we used both *in vitro* shRNA mediated inhibition and pharmacologic inhibition to demonstrate that IKBKE expression and activity is necessary for Ewing sarcoma cell survival and anchorage independent growth.

Additionally, Ewing sarcoma cell lines were highly responsive to two inhibitors (MRT67307, CYT387) of IKBKE/TBK1, which both demonstrated on-target activity *in vitro* and *in vivo*. Treatment of NSG mice with Ewing sarcoma xenografts with 100 mg/kg daily of CYT387 (a clinically approved JAK1/2 inhibitor with activity against IKBKE/TBK1) resulted in significantly impaired tumor growth and improved survival without any noted toxicity.

However, pharmacologic on target activity as assessed by p-TBK1 S172 was only marginally elevated at the end of 20 and 27 days of treatment, suggesting that higher doses of CYT387 may be necessary to obtain optimal target inhibition or that resistance to therapy may

have developed at the dose and schedule tested. A second Ewing sarcoma xenograft study with a three-arm design, including vehicle treatment and two doses of CYT387, including treatment at the maximum tolerated dose, is warranted.

We have also demonstrated a potential mechanism of CYT387 activity in Ewing sarcoma. We observed that chemical inhibition with CYT387 in a highly sensitive Ewing sarcoma line resulted in impairment of nuclear localization of NF-κB family proteins RelA/p65 and c-Rel, corresponding with attenuation of IκBα degradation following stimulation with TNF-α. Further, in contrast to parthenolide inhibition in TC32 cells, we also noted impairment in nuclear localization of the mature form of NF-κB1 (p50).

These results suggest that the pharmacologic mechanism of action of CYT387 in Ewing sarcoma cells involves impairment of NF-κB activation through inhibition of upstream IKK activity. While CYT387 has been shown to be an inhibitor of the non-canonical IKKs, further experimentation is necessary to demonstrate whether CYT387 specifically targets the non-canonical IKK pathway, or whether it also inhibits IKBKB activity, as the markers we evaluated for impairment of NF-κB activation are downstream of both the canonical and non-canonical NF-κB pathways.

Additionally, we also showed that CYT387 and MRT67307 inhibition of IKBKE/TBK1 did not inhibit downstream Akt phosporylation but that it did engender cytotoxic stress that resulted in elevated PARP-1 cleavage and DNA damage, with elevations in pH2A.X as well as subsequent induction of apoptosis.

Implications for future directions focused on the role of IKBKE in Ewing sarcoma

Future experiments will focus on characterizing the mechanisms of IKBKE activation in Ewing sarcoma as well as the contribution of IKBKE to Ewing sarcoma cell survival as compared to TBK1 and other canonical IKK proteins.

A recent study by Zhu et. al. has demonstrated a unique role of CYT387 in inhibition of an autocrine signaling loop involved in activating IKBKE/TBK1 in *KRAS*-dependent tumors. The study authors demonstrated that IKK-related kinases promote *KRAS*-driven tumorigenesis through the activation of an autocrine loop involving IL-6 and CCL5 which activates STAT3 and induces of IKBKE/TBK1 resulting in positive feedback with increased expression of CCL5 and IL-6 cytokines.[43] This autocrine loop was effectively impaired with CYT387 treatment. The potential role of CCL5 and IL-6 expression in autocrine stimulation of IKBKE expression in Ewing sarcoma will be investigated, as will the effects of CYT387 treatment on impairing expression of CCL5 and IL-6.

Furthermore, we will evaluate the dysregulation of IKBKE-specific downstream phosphorylation targets, such as CYLD as well as TRAF2 phosphorylation, in the context of chemical perturbation by CYT387 and MRT67307 and shRNA mediated knockdown of IKBKE, to evaluate whether these pathways which were demonstrated to be necessary in breast cancer tumorigenesis are also similarly important in Ewing sarcoma.

Additionally, since IKBKE function can overlap with the catalytic canonical IKK proteins, we will further investigate the dependence of Ewing cells on these related proteins and subsequent perturbation of NF-κB signaling following shRNA mediated knockdown of these proteins. Notably, IKBKB did score highly in our near whole genome shRNA screen, although not as highly as IKBKE. To further investigate the contribution of IKBKE to cell survival and NF-κB signaling in Ewing sarcoma, relative to canonical NF-κB signaling, we plan to develop CRISPR-Cas9 mediated knockouts of IKBKE in Ewing sarcoma cell lines and evaluate the impact of IKBKE knockouts on cell survival and on NF-κB signaling, IκBα stabilization, NF-κB p65 phosphorylation, c-Rel nuclear localization and IKBKE downstream targets, in the setting of

endogenous canonical IKK expression. We can further evaluate whether loss of IKBKE can be rescued with expression of TBK1 or other catalytic IKK proteins.

Further, in the near term, small molecule inhibitors of NF-κB signaling can be utilized to evaluate if there are potential overlapping dependencies of Ewing sarcoma cells on the canonical and non-canonical IKK pathways. For example, we observed that treatment of Ewing sarcoma cells with parthenolide, an inhibitor of IKBKB, and CYT387, an inhibitor of IKBKE/TBK1, resulted in substantial but not complete impairment of NF-κB nuclear localization by either of these inhibitors and combined inhibition of the parallel canonical and non-canonical IKKs with these small molecules may be additive or synergistic and should be further evaluated *in vitro*.

While we have demonstrated that IKBKE is an essential gene for Ewing sarcoma cell survival, these future experiments are necessary to facilitate our understanding of potential autocrine mechanisms for IKBKE activation in Ewing sarcoma and to evaluate the contributions of canonical and non-canonical NF-κB pathway proteins to the malignant growth of Ewing sarcoma tumors.

The role of G1 regulation in Ewing sarcoma

Through a near whole genome shRNA screen, we have demonstrated that G1 cell cycle regulation, namely the activity of cyclin D1 and CDK4, are particularly important in the context of cells expressing EWS/FLI1 as compared to other non-similar cancer types. This functional genomic data is corroborated by a screen of seven hundred cancer cell lines in which EWS/FLI1 expressing lines were significantly more sensitive to the CDK 4/6 inhibitor PD-0332991 than other tumor types.[47] Overall sensitivity of Ewing tumors to CDK4/6 inhibition may in part be related to the role of EWS/FLI1 in directly activating *CCND1* gene transcription, resulting in increased cyclin D1 expression as compared to other cancer cell lines.

We demonstrated that knockdown of cyclin D1 and CDK4 results in impaired cell viability and anchorage independent growth in two Ewing sarcoma cell lines. Notably, there was increased sensitivity of TC32 to shRNA mediated knockdown of cyclin D1 and CDK4 as compared to TC71. This relationship was preserved on pharmacologic inhibition of CDK4 with a highly specific CDK 4/6 inhibitor, LEE011. The data presented show that treatment of Ewing sarcoma cell lines with LEE011 results in impairment of Rb phosphorylation and significant G1 cell cycle arrest as well as apoptosis in a panel of highly sensitive lines.

Finally, *in vivo* treatment of mouse xenografts with LEE011 demonstrates that this is a potential therapeutic strategy for the treatment of Ewing sarcoma. NSG mice with xenografts treated at 75 mg/kg/day and 250 mg/kg/day experienced rapid and significant attenuation of tumor growth with regression noted in the highest dose arm. The compound was well tolerated at the 75 mg/kg/day dose, although mice in the 250 mg/kg/day arm did experience some toxicity. This study is ongoing and evaluation of effects of treatment on survival, pharmacodynamics, and immunohistochemical staining for markers of cell proliferation and apoptosis will be performed on completion of this study.

We also show that sensitivity to LEE011 mediated CDK4 inhibition is not related to variable p16 expression as p16 loss is frequent in the majority of cell lines and p16 expression is low throughout the panel of Ewing sarcoma lines tested. A similar pattern of loss was noted with CDK2NB. While we noted that at the RNA Rb expression was lower in Ewing lines with decreased sensitivity to the drug, endogenous p-Rb levels were similarly elevated in the two most highly sensitive and least sensitive lines (Figure 8E). Additionally, CDK4 and cyclin D1 expres sion are uniformly elevated across the Ewing sarcoma lines. We did note that expression of the oncogenic variant of cyclin D1b as compared to cyclin D1a expression was inversely correlated with sensitivity to LEE011. We plan to further test this hypothesis by inducing

overexpression of cyclin D1b in highly sensitive cell lines and cyclin D1a in less sensitive lines and test the effects on cell viability following LEE011 treatment.

Cell cycle arrest as a therapeutic strategy in cancer

Inhibition of cell cycle progression through attenuation of CDK activity has long been a therapeutic target in cancer, as numerous genetic and epigenetic events result in aberrant activity of these proteins.[58,59] Pre-clinical data from the testing of cell cycle inhibitors has demonstrated potent cytostatic effects, some apoptotic effects and even tumor xenograft regression associated with certain pan-CDK inhibitors like flavopiridol.[60]

However, the therapeutic strategy of cell cycle inhibition has not always yielded results in phase I and II trials. For example, Flavopiridol, a pan-CDK inhibitor with activity against cdk1, cdk2, cdk4 and cdk7 was shown to induce cell cycle arrest accompanied by apoptosis in non-small cell lung cancer lines in a p53 independent manner and subsequently was shown to induce tumor regression in many solid tumor xenografts.[60] It became the first CDK inhibitor to reach clinical trial with disappointing results, prolonging the duration of stable disease in some groups of patients, and inducing no notable responses to therapy as a single agent.[58]

Subsequent work has shown sequence specific treatment of cancer with chemotherapeutics and cell cycle inhibitors can provide synergy. For example, recruitment of cells to the S-phase following pretreatment of cells with non-cytotoxic concentrations of chemotherapeutics sensitized cells to subsequent flavopiridol induced apoptosis in an E2F dependent manner.[61]

There has been additional development of highly specific CDK inhibitors. CDK 4/6 inhibitor PD-0332991 was one of the first CDK 4/6 inhibitors to reach clinical trial. Pre-clinically, it was shown to have anti-proliferative effects on Rb-positive tumor cells and resulted in tumor regression of human colon carcinoma xenografts.[62] LEE011, another highly specific

CDK 4/6 inhibitor, has recently been shown in pre-clinical models of neuroblastoma to induce cytostasis and xenograft growth delay, with increased sensitivity noted in neuroblastoma cell lines with *MYCN* amplification.[63]

Recently, preliminary results from a randomized phase II study of PD-0332991 in combination with letrozole versus letrozole alone in patients with ER+/HER2- advanced breast cancer showed significant improvement in progression free survival from 7.5 months to 26.1 months, suggesting synergy between hormone receptor inhibition and cell cycle inhibition that was seen in pre-clinical evaluations of PD-0332991 with tamoxifen.[63,64]

The promising results of the combination therapy strategy involving PD-0332991 and letrozole, highlight the importance of identifying synergistic relationships between CDK inhibitors and standard chemotherapies to derive maximal survival benefits. Furthermore, design of optimal therapeutic combinations must take into consideration the role of CDK inhibition in inducing pharmacologic quiescence, which can engender resistance to traditional cytotoxic chemotherapy and radiation therapy when used in combination.[65]

This has been shown in pre-clinical models in which treatment with CDK 4/6 inhibitors prior to treatment with DNA-damaging agents results in attenuation of DNA damage.[65] Pharamacologic quiescence was also seen *in vivo* in genetically engineered models of HER2 driven breast cancer. Tumor bearing mice were treated with PD-0332991 co-administered with carboplatin, which resulted in *in vivo* tumor protection, while both carboplatin and the CDK 4/6 inhibitor, had activity against the tumor as single agents.[66]

In Ewing, LEE011 has resulted in induction of apoptosis in highly sensitive cell lines, there remain a large fraction of cells under G1 arrest that exist in a state of pharmacologic quiescence. Additional pre-clinical testing of sequence specific synergy or antagonism between cytotoxic chemotherapy and CDK 4/6 inhibition would help inform the development of clinical

trials to treat patients with relapsed or metastatic Ewing sarcoma in combination with standard chemotherapy regimens. We are currently working in collaboration with the National Center for Advancing Translational Sciences (NCATS) at the National Institutes of Health, to conduct high throughput screening of sequence-specific combination regimens involving Ewing based cytotoxic chemotherapy (adriamycin, vincristine, cyclphosphamide, ifosfamide and etoposide) and Ewing specific targeted therapies, such as IGF-1R, mTOR/PI-3K and FAK inhibitors, followed by treatment with PD-0332991 to identify potential synergistic regimens that can be subsequently validated *in vivo* and inform future clinical trial design for the translation of this inhibitor to the clinic in the treatment of patients with Ewing sarcoma.

Implications for therapy of Ewing sarcoma

Through the use of a near-whole genome shRNA depletion screen we have identified and characterized novel targetable liabilities for the treatment of Ewing sarcoma. These targetable liabilities, IKBKE and CDK4, highlight aspects of Ewing sarcoma tumor biology, notably a dependence of NF-κB signaling and EWS/FLI1 associated sensitivity to CDK4/6 inhibition. Pharmacologic inhibitors for both IKBKE (CYT387) and CDK4/6 (LEE011) are in clinical trials for other neoplasms and have shown efficacy in pre-clinical xenograft models for Ewing supporting the need to identify highly effective drug combinations with these new targeted therapies and the potential for rapid translation of these inhibitors for clinical evaluation in the treatment of patients with Ewing sarcoma.

Summary

Ewing sarcoma is the second most common bone tumor that predominantly affects children and young adults. Advances in treatment regimens have improved survival for patients with localized disease, yielding survival rates of 75% for individuals who receive multi-modality therapy with radiation or surgery and a chemotherapy regimen including adriamycin, vincristine, and cytoxan alternating with ifosfamide or etoposide. Despite multi-modality therapy, patients with relapsed or metastatic disease have poor survival, underlying the need for the development of targeted therapies.

The biology of Ewing sarcoma is primarily mediated by the expression of a fusion protein, either EWS/FLI1 or EWS/ERG, formed by the fusion of chromosome 11 and 22 or chromosome 21 and 22. The fusion of EWS with transcription factors FLI1 or ERG, results in aberrant gene expression with dual activation of oncogenes and repression of tumor suppressor genes, enabling transformation of the Ewing precursor cell.

To identify genes that promote cell survival and oncogenesis in an EWS/FLI1 dependent manner, we performed a genome wide screen to detect genes whose loss results in Ewing sarcoma cell death. The list of top genes from this screen was then prioritized based on expression in Ewing cell lines and tumors and compared to essential genes in similar and non-similar cancers to prioritize gene targets whose loss is preferentially lethal in the context of EWS/FLI1 expression. We identified a gene involved in NF-κB signaling, IKBKE and mediators of G1 cell cycle progression (CDK4 and CCND1) as essential in the context of Ewing sarcoma. Next, we showed through genetic suppression of gene expression that IKBKE, CDK4 and CCND1 are necessary for Ewing sarcoma cell survival. These results were confirmed by pharmacologic inhibition of these targets. Additionally, we showed that treatment of Ewing sarcoma cells with small molecule inhibitors of IKBKE resulted in impaired nuclear

translocation of NF-κB transcription factors, which promote cell survival and proliferation signals. Additionally, inhibition of CDK4 resulted in decreased phosphorylation of the downstream tumor suppressor target Rb that then impairs progression of cells through the cell cycle inducing arrest of cell division at the G1 checkpoint. Finally, we demonstrated *in vivo* that inhibition of IKBKE and CDK4 with small molecule inhibitors resulted in impairment of tumor growth, suggesting that these targets should be further explored for clinical translation and development of novel therapies for patients with Ewing sarcoma.

Acknowledgements:

Over the past year, I have been privileged to work in the laboratory of Dr. Kim Stegmaier. I have benefitted from her continual support, coaching and mentorship. Kim's unyielding dedication to her patients, passion for science and those she mentors is motivating and serves as inspiration for the type of physician-scientist career I hope to have. During my time in her lab, she has taught me how to approach clinically relevant, basic science questions with rigor and creativity, to write and communicate science more effectively and most importantly, how to be a kind and gracious mentor.

I have also benefitted from the opportunity to learn from and collaborate with the many amazing members of our lab. Namely, this work would not have been possible without a few individuals who I wish to acknowledge. Aaron Thorner, PhD not only trained me in basic laboratory techniques when I joined the lab but also initiated the Ewing sarcoma whole genome shRNA screen several years before I started in the lab. I am also thankful for Gabriela Alexe, PhD for lending her computational biology expertise to helping us analyze and interpret the whole genome shRNA data from the Achilles project to identify the most biologically relevant genes to target in Ewing sarcoma. Alyssa Kennedy, MD PhD, and Liying Chen, PhD, have been invaluable friends and colleagues who I have worked closely with on evaluating the role of LEE011 in Ewing sarcoma. Alyssa completed the CDK4 and CCND1 gene knockdown experiments presented within this thesis and Liying is lending her expertise in chromatin biology to understanding CCND1 gene regulation in Ewing sarcoma. I also wish to thank Dr. David Barbie for providing us with IKBKE /TBK1 inhibitors and many helpful discussions regarding the biology of these oncogenes.

I must also thank the many members of our lab, Brian Crompton, Neil Mehta, Elizabeth Hwang, Alex Puissant, Angela Su, Giovanni Roti, Yana Pikman, Linda Ross, Chris Bassil and

Alli O'Neill, for providing a collaborative, fun and warm environment and being incredibly inspiring colleagues.

Howard Hughes Medical Institute provided the funding to complete a year immersed in the lab, an opportunity for which I will always be grateful. In particular, Melanie Daub's stewardship of the fellowship program provided for numerous mentorship opportunities to envision and build the career I hope to have as a physician-scientist.

I am also thankful for my clinical mentors at Harvard Medical School. In particular, Dr. Anthony D'Amico has been a continual presence throughout my years as a member of Holmes Society and has been a trusted source of counsel, guiding me as I have made several important career and life decisions. I and the many students of Holmes society are truly blessed to have his guidance and support.

Most importantly, I cannot conclude without giving the utmost gratitude for the unyielding love and support of my mother and grandparents. Their faith in my abilities and sacrifices for my education are the bedrock of my accomplishments.

References:

1. Esiashvili N, Goodman M, Marcus RB, Jr. Changes in incidence and survival of Ewing sarcoma patients over the past 3 decades: Surveillance Epidemiology and End Results data. *J Pediatr Hematol Oncol.* Jun 2008;30(6):425-430.

2. Stahl M, Ranft A, Paulussen M, et al. Risk of recurrence and survival after relapse in patients with Ewing sarcoma. *Pediatr Blood Cancer.* Oct 2011;57(4):549-553.

3. Grier H. The Ewing family of tumors. Ewing's sarcoma and primitive neuroectodermal tumors. *Pediatr Clin North Am.* 1997;44(4):991.

4. Delattre O, Zucman J, Melot T, et al. The Ewing family of tumors--a subgroup of small-round-cell tumors defined by specific chimeric transcripts. *N Engl J Med.* Aug 4 1994;331(5):294-299.

5. Delattre O, Zucman J, Plougastel B, et al. Gene fusion with an ETS DNA-binding domain caused by chromosome translocation in human tumours. *Nature.* Sep 10 1992;359(6391):162-165.

6. Bailly RA, Bosselut R, Zucman J, et al. DNA-binding and transcriptional activation properties of the EWS-FLI-1 fusion protein resulting from the t(11;22) translocation in Ewing sarcoma. *Mol Cell Biol.* May 1994;14(5):3230-3241.

7. Sorensen PH, Lessnick SL, Lopez-Terrada D, Liu XF, Triche TJ, Denny CT. A second Ewing's sarcoma translocation, t(21;22), fuses the EWS gene to another ETS-family transcription factor, ERG. *Nat Genet.* Feb 1994;6(2):146-151.

8. May WA, Gishizky ML, Lessnick SL, et al. Ewing sarcoma 11;22 translocation produces a chimeric transcription factor that requires the DNA-binding domain encoded by FLI1 for transformation. *Proc Natl Acad Sci U S A.* Jun 15 1993;90(12):5752-5756.

9. Prieur A, Tirode F, Cohen P, Delattre O. EWS/FLI-1 silencing and gene profiling of Ewing cells reveal downstream oncogenic pathways and a crucial role for repression of insulin-like growth factor binding protein 3. *Mol Cell Biol.* Aug 2004;24(16):7275-7283.

10. Tanaka K, Iwakuma T, Harimaya K, Sato H, Iwamoto Y. EWS-Fli1 antisense oligodeoxynucleotide inhibits proliferation of human Ewing's sarcoma and primitive neuroectodermal tumor cells. *J Clin Invest.* Jan 15 1997;99(2):239-247.

11. Arvand A, Denny CT. Biology of EWS/ETS fusions in Ewing's family tumors. *Oncogene.* Sep 10 2001;20(40):5747-5754.

12. Mendiola M, Carrillo J, Garcia E, et al. The orphan nuclear receptor DAX1 is up-regulated by the EWS/FLI1 oncoprotein and is highly expressed in Ewing tumors. *Int. J. Cancer.* 2006;118:1381-1389.

13. Kinsey M, Smith R, Iyer AK, McCabe ER, Lessnick SL. EWS/FLI and its downstream target NR0B1 interact directly to modulate transcription and oncogenesis in Ewing's sarcoma. *Cancer Res.* Dec 1 2009;69(23):9047-9055.

14. Rocchi A, Manara MC, Sciandra M, et al. CD99 inhibits neural differentiation of human Ewing sarcoma cells and therby contributes to oncogenesis. *The Journal of Clinical Investigation.* 2010;120(3):668-680.

15. Nishimori H, Sasaki Y, Yoshida K, et al. The Id2 gene is a novel target of transcriptional activation by EWS-ETS fusion proteins in Ewing family tumors. *Oncogene* 2002;21:8302-8309.

16. Zhang J, Hu S, Schofield DE, Sorensen PH, Triche TJ. Selective usage of D-Type cyclins by Ewing's tumors and rhabdomyosarcomas. *Cancer Res.* Sep 1 2004;64(17):6026-6034.

17. Paronetto MP, Minana B, Valcarcel J. The ewing sarcoma protein regulates DNA damage-induced alternative splicing *Molecular Cell.* 2011;43:353-368.

18. Sanchez G, Delattre O, Auboeuf D, Dutertre M. Coupled alteration of transcription and splicing by a single oncogene: boosting the effect on cyclin D1 activity. *Cell Cycle.* Aug 2008;7(15):2299-2305.
19. Sanchez G, Bittencourt D, Laud K, et al. Alteration of cyclin D1 transcript elongation by a mutated transcription factor up-regulates the oncogenic D1b splic isoform in cancer. *Proc. Natl. Acad. Sci.* 2008;105(16):6004-6009.
20. Matsumoto Y, Tanaka K, Nakatani F, Matsunobu T, Matsuda S, Iwamoto Y. Downregulation and forced expression of EWS-Fli1 fusion gene results in changes in the expression of G1 regulatory genes. *British Journal of Cancer.* 2001;84(6):768-775.
21. Kovar H, Jug G, Aryee DN, et al. Among genes involved in the RB dependent cell cycle regulatory cascade the p16 tumor suppressor gene is frequently lost in the Ewing family of tumors. *Oncogene.* 1997;15:2225-2232.
22. Karin M, Cao Y, Greten FR, Li ZW. NF-kB in cancer: from innocent bystander to major culprit. *Nature Reviews Cancer.* 2002;2:301-310.
23. Guo JP, Coppola D, Cheng JQ. IKBKE protein activates Akt independent of phosphatidylinositol 3-kinase/PDK1/mTORC2 and the pleckstrin homology domain to sustain malignant transformation. *J Biol Chem.* Oct 28 2011;286(43):37389-37398.
24. Ou YH, Torres M, Ram R, et al. TBK1 directly engaged Akt/PKB survival signaling to support oncogenic transformation. *Molecular Cell.* 2011;41(4):458-470.
25. Clark K, Peggie M, Plater L, et al. Novel cross-talk within the IKK family controls innate immunity *Biochem. J.* . 2011;434:93-104.
26. Barbie DA, Tamayo P, Boehm JS, et al. Systematic RNA interference reveals that oncogenic KRAS-driven cancers require TBK1. *Nature.* 2009;462(7269):108-112.
27. Boehm JS, Zhao JJ, Yao J, et al. Integrative genomic approaches identify IKBKE as a breast cancer oncogene. *Cell.* 2007;129(6):1065-1079.
28. Javelaud D, Wietzerbin J, Delattre O, Besancon F. Induction of p21Waf1/Cip1 by TNFalpha requires NF-kappaB activity and antagonizes apoptosis in Ewing tumor cells. *Oncogene.* Jan 6 2000;19(1):61-68.
29. Javelaud D, Poupon M, Wietzerbin J, Besancon F. Inhibition of constitutive NF-kB activity suppresses tumorigenicity of Ewing sarcoma EW7 cells. *Int. J. Cancer.* 2002;98:193-198.
30. Oikawa T. ETS transcription factors: possible targets for cancer therapy. *Cancer Sci.* Aug 2004;95(8):626-633.
31. Garnett MJ, Edelman EJ, Heidorn SJ, et al. Systematic identification of genomic markers of drug sensitivity in cancer cells. *Nature.* Mar 29 2012;483(7391):570-575.
32. Brenner JC, Feng FY, Han S, et al. PARP-1 Inhibition as a targeted strategy to treat Ewing's sarcoma. *Cancer Research.* 2012;72(7):1608-1613.
33. Cheung HW, Cowley GS, Weir BA, et al. Systematic investigation of genetic vulnerabilities across cancer cell lines reveals lineage-specific dependencies in ovarian cancer. *Proc Natl Acad Sci U S A.* Jul 26 2011;108(30):12372-12377.
34. von Levetzow C, Jiang X, Gwye Y, et al. Modeling initiation of Ewing sarcoma in human neural crest cells. *PLoS One.* 2011;6(4):e19305.
35. Owen LA, Lessnick SL. Identification of target genes in their native cellular context: an analysis of EWS/FLI in Ewing's sarcoma. *Cell Cycle.* 2006;5(18):2049-2053.
36. Reich M, Liefeld T, Gould J, Lerner J, Tamayo P, Mesirov JP. GenePattern 2.0. *Nature Genetics.* 2006;38(5):500-501.
37. Luo B, Cheung HW, Subramanian A, et al. Highly parallel identification of essential genes in cancer cells. *Proc Natl Acad Sci U S A.* Dec 23 2008;105(51):20380-20385.

38. Shen RR, Hahn WC. Emerging roles for the non-canonical IKKs in cancer. *Oncogene.* Feb 10 2011;30(6):631-641.

39. Baldwin AS. Regulation of cell death and autophagy by IKK and NF-kB: critical mechanisms in immune function and cancer. *Immunological Reviews.* 2012;246:327-345.

40. Renner F, Moreno R, Schmitz ML. SUMOylation-dependent localization of IKKe in PML nuclear bodies is essential for protection against DNA-damage-triggered cell death. *Molecular Cell.* 2010;37:503-515.

41. Tyner JW, Bumm TG, Deininger J, et al. CYT387, a novel JAK2 inhibitor, induces hematologic responses and normalizes inflammatory cytokines in murine myeloproliferative neoplasms. *Blood.* Jun 24 2010;115(25):5232-5240.

42. Monaghan KA, Khong T, Burns CJ, Spencer A. The novel JAK inhibitor CYT387 suppresses multiple signalling pathways, prevents proliferation and induces apoptosis in phenotypically diverse myeloma cells. *Leukemia.* Dec 2011;25(12):1891-1899.

43. Zhu S, Aref AR, Cohoon TJ, et al. Inhibition of KRAS-driven tumorigenicity by interruption of an autocrine cytokine circuit. *Cancer Discovery.* 2014.

44. Harris J, Oliere S, Sharma S, et al. Nuclear accumulation of cRel following C-terminal phosphorylation by TBK1/IKKe. *The Journal of Immunology.* 2006;177:2527-2535.

45. CYT387 KINOMEscan-Dataset-HMS LINCS Database. http://lincs.hms.harvard.edu/db/datasets/20082/. Accessed January 12, 2014.

46. Sherr CJ, Roberts JM. Living with or without cyclins and cyclin-dependent kinases. *Genes Dev.* 2004;18:2699-2711.

47. Yang W, Soares J, Greninger P, et al. Genomics of drug sensitivity in cancer (GDSC): a resource for therapeutic biomarker discovery in cancer cells. *Nucleic Acids Research.* 2012;41:D955-D961.

48. Konecny GE, Winterhoff B, Kolarova T, et al. Expression of p16 and Retinoblastoma determines response to CDK4/6 ihibition in ovarian cancer. *Clinical Cancer Research.* 2011;17(6):1591-1602.

49. Miller EKA, Dean JL, McNeil CM, et al. Cyclin D1b protein expression in breast cancer is independent of cyclin D1a and associated with poor disease outcome. *Oncogene.* 2009;28:1812-1820.

50. Riggi N, Suva ML, Suva D, et al. EWS-FLI-1 expression triggers a Ewing's sarcoma initiation program in primary human mesenchymal stem cells. *Cancer Research.* 2008;68(7):2176-2185.

51. McKinsey EL, Parrish JK, Irwin AE, et al. A novel oncogenic mechanism in Ewing sarcoma involving IGF pathway targeting by EWS/Fli1-regulated microRNAs. *Oncogene.* 2011;30:4910-4920.

52. Li Y, Tanaka K, Fan X, et al. Inhibition of the transcriptional function of p53 by EWS-Fli1 chimeric protein in Ewing family tumors. *Cancer Letters.* 2010;294(1):57-65.

53. Adli M, Baldwin AS. IKKi/IKKe controls constitutive cancer cell-associated NF-kB activity via regulation of Ser-536 p65/RelA phosphorylation. *The Journal of Biological Chemistry.* 2006;281:26976-26984.

54. Eddy SF, Guo S, Demicco EG, et al. Inducible IkB kinase/ IkB kinase epsilon expression is induced by CK2 and promoted aberrant nuclear factor-kB activation in breast cancer cells. *Cancer Research.* 2005;65:11375-11383.

55. Hutti JE, Shen RR, Abbott DW, et al. Phosphorylation of the tumor suppressor CYLD by the breast cancer oncogene IKKe promotes cell transformation. *Molecular Cell.* 2009;34(4):461-472.

56. Zhou AY, Shen RR, Kim E, et al. IKKe-mediated tumorigenesis requires K63-Linked polyubiquitination by a cIAP1/cIAP2/TRAF2 E3 Ubiquitin ligase complex. *Cell Reports.* 2013;3:1-10.
57. Shen RR, Zhou AY, Kim E, Lim E, Habelhah H, Hahn WC. IkB kinase E phosphorylates TRAF2 to promote mammary epithelial cell transformation. *Molecular and Cellular Biology.* 2012;32(23):4756-4768.
58. Shapiro GI. Preclinical and clinical development of the cyclin-dependent kinase inhibitor flavopiridol. *Clinical Cancer Research.* 2004;10:4270-4275.
59. Shapiro GI. Cyclin-dependent kinase pathways as targets for cancer treatment *Journal of Clinical Oncology.* 2006;24(11):1770-1783.
60. Shapiro GI, Koestner DA, Matranga CB, Rollins BJ. Flavopiridol induces cell cycle arrest and p53-independent apoptosis in non-small cell lung cancer cell lines. *Clinical Cancer Research.* 1999;5:2925-2938.
61. Jiang J, Matranga CB, Cai D, et al. Flavopiridol-induced apoptosis during S phase requires E2F-1 and inhibition of cyclin A-dependnet kinase activity. *Cancer Research.* 2003;63:7410-7422.
62. Fry DW, Harvey PJ, Keller PR, et al. Specific Inhibition of cyclin-dependent kinase 4/6 by PD 0332991 and associated antitumor activity in human tumor xenografts. *Mol Cancer Ther.* 2004;3:1427-1438.
63. Rader J, Russell MR, Hart LS, et al. Dual CDK4/6 inhibition induces cell-cycle arrest and senescence in Neuroblastoma. *Clinical Cancer Research.* 2013;19:6173-6182.
64. Finn RS, Crown JP, Lang I, et al. Results of a randomized phase 2 study of PD 0332991, a cyclin-dependent kinase (CDK) 4/6 inhibitor in combination with letrozole versus letrozole alone for first-line treatment of ER+/HER2- advanced breast cancer. *Cancer Research.* 2012;72(24):Supplement 3.
65. Dean JL, McClendon K, Knudsen ES. Modification of the DNA damage response by therapeutic CDK 4/6 inhibition *The Journal of Biological Chemistry.* 2012;287:29075-29087.
66. Roberts PJ, Bisi JE, Strum JC, et al. Multiple roles of cyclin-dependent kinase 4/6 inhibitors in cancer therapy. *Journal of the National Cancer Institute.* 2012;104(6):476-487.

Tables and Figures:

Figure 1: IKBKE scores as a top hit in a near-whole genome shRNA screen of Ewing cell lines. A,B. Targeting of IKBKE, IKBKB, and NF-κB1, with shRNAs resulted in preferential depletion of Ewing sarcoma cells as compared to non-similar cell lines. C. IKBKE is expressed in the majority of Ewing sarcoma cell lines, as a doublet, at levels similar to MCF-7, a breast cancer cell line with dependency on IKBKE.

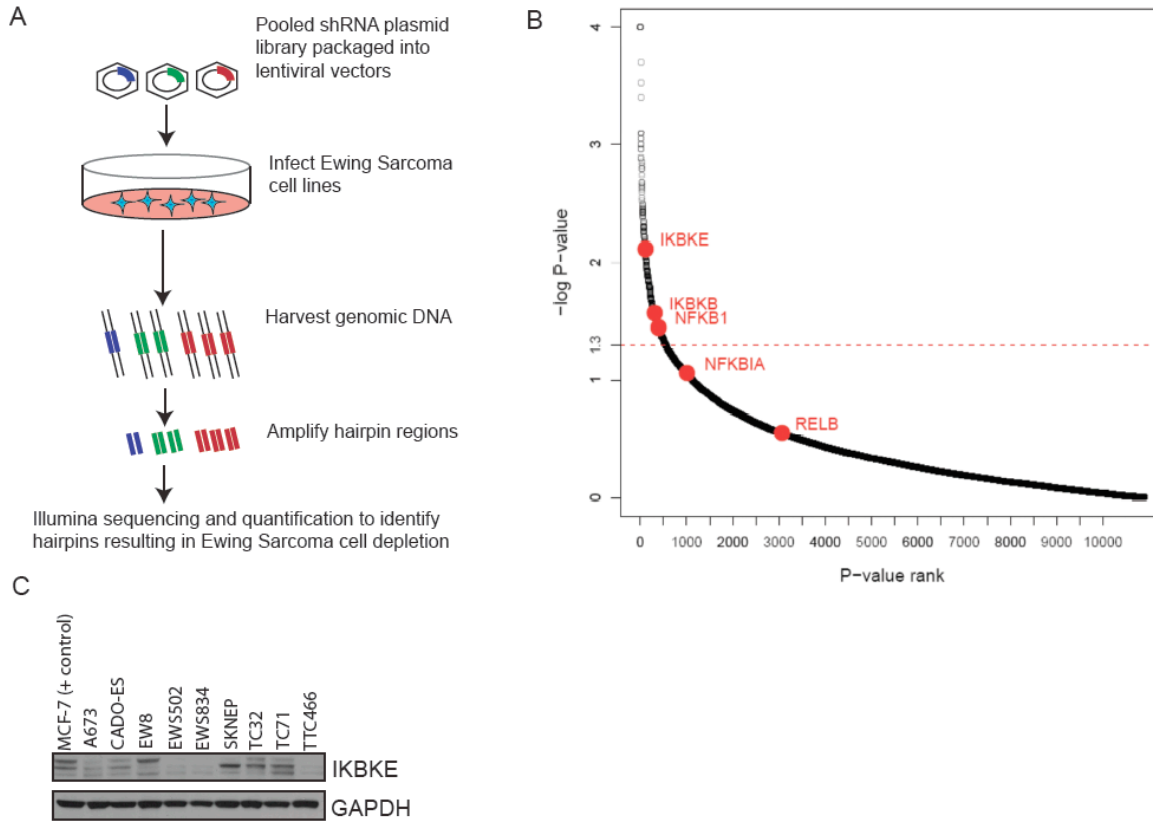

Figure 2: Suppression of IKBKE impairs cell growth and colony formation.
A. Panels showing decreased levels of IKBKE after infection of Ewing sarcoma cell lines with three unique shRNAs targeting the transcript and corresponding impairment in Ewing sarcoma cell growth. Cell growth was measured using a luminescent ATP detection assay and relative luminescence was calculated by dividing each timepoint's luminescent value by the average day 0 luminescent value for each hairpin. B. Colony formation in methylcellulose relative to control shRNA. Shown are the means of 14 replicates for viability and 2 replicates for colony formation +/- SEM, p-values calculated with student's t-Test.

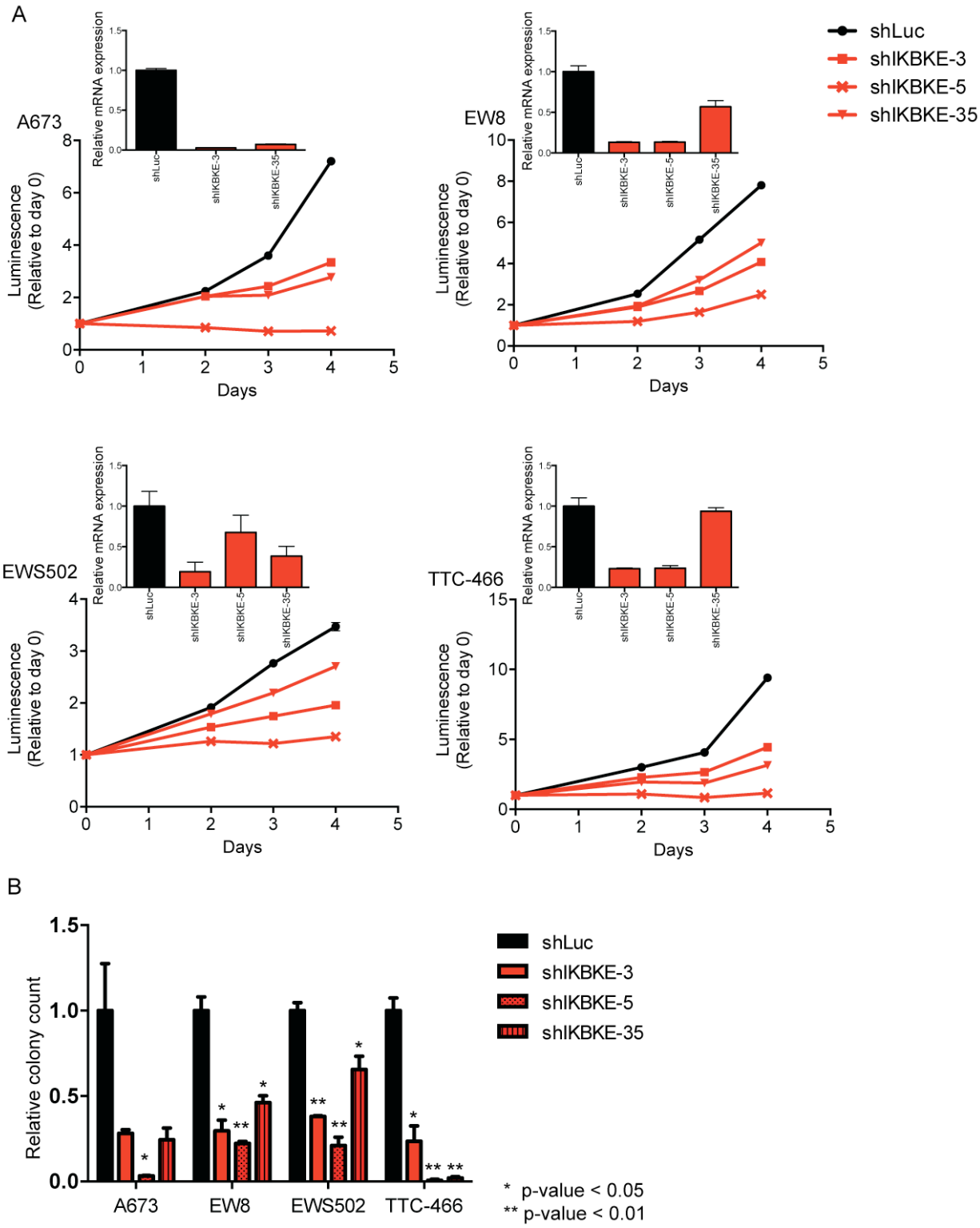

Figure 3: Small molecule inhibitors of IKBKE/TBK1 impair Ewing Sarcoma cell growth and colony formation and induce PARP-1 cleavage. A, B, C. Effects of five days of treatment with MRT67307 (IKBKE/TBK1 inhibitor), CYT387 (JAK1/2 and IKBKE/TBK1 inhibitor), and Ruxolitinib (JAK1/2 inhibitor) on Ewing sarcoma cell lines. Cells lines were responsive to CYT387 and MRT67307 but not to the JAK1/2 inhibitor, Ruxolitinib. D. CYT387 inhibits colony formation in a dose dependent fashion. E. CYT387 (5 μM) and MRT67307 (1.5 μM) have on-target activity in Ewing TC32 cells, with inhibition of IKBKE/TBK1 as demonstrated by paradoxical elevation of p-TBK (S172). F. CYT387 and MRT67307 do not significantly inhibit AKT phosphorylation, as compared to Akt inhibitor MK-2206 and PI-3K GDC-0941, but there is elevation in markers of cytotoxicity and DNA damage evidenced by elevations in pH2A.X and PARP-1 cleavage after treatment with 5 μM of compound for 24 hours. G. To evaluate effects of IKBKE/TBK1 inhibition on NF-κB signaling in Ewing, TC32 cells were incubated with CYT387 for six hours prior to stimulation with TNF-α (30 ng/mL). IκBα degradation was measured by harvesting TC32 cells thirty minutes after stimulation with TNF-α. TNF-α stimulation resulted in degradation of IκBα, and this effect was attenuated with CYT387 treatment. Parthenolide, an inhibitor of IκBα phosphorylation was used as a positive control. Similar effects of CYT387 activity were seen in HEK-293T cells which also express IKBKE.[53] Nuclear extracts were prepared from TC32 cells harvested following forty-five minutes of TNF-α stimulation. Treatment with CYT387 resulted in decreased nuclear localization of NF-κB family proteins RelA/p65 and c-Rel. There was a modest impairment of p50 nuclear localization as compared to parthenolide and DMSO controls and no change in p52 nuclear localization. RelB (not shown) is not expressed in TC32 cells.

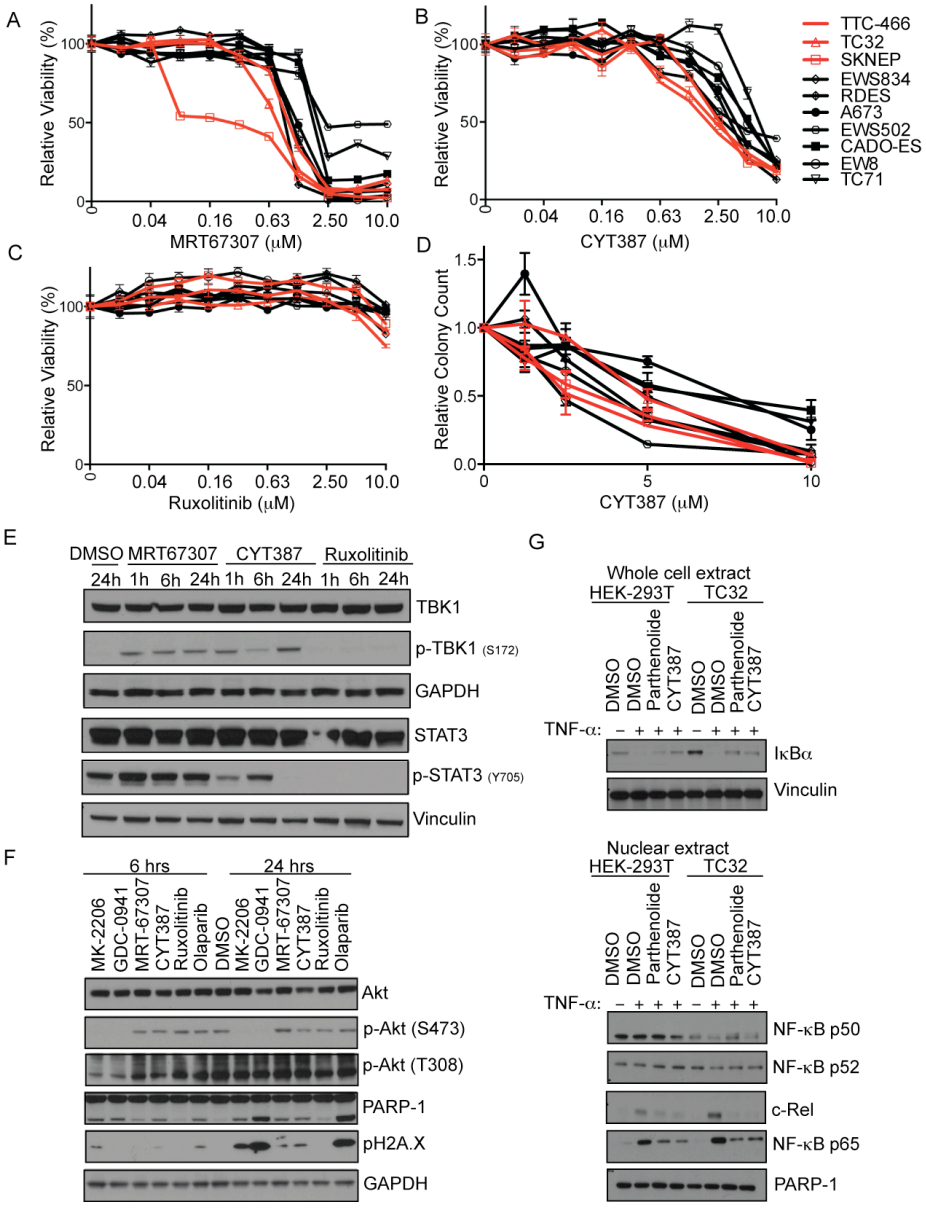

Figure 4: Treatment of Ewing sarcoma with CYT387 results in induction of apoptosis but no cell cycle arrest. A. Effects 72 hours of CYT387 treatment on SKNEP, TC32, and TC71 demonstrate induction of apoptosis (* p-value = 0.02, ** p-value <0.01). B. CYT387 treatment does result in off-target inhibition of CDK4, with downstream dephosphorylation of p-Rb (S780) as compared to the CDK 4,6 inhibitor LEE011. C. Despite dephosphorylation of p-Rb (S780), there is no corresponding G1 arrest, but there is a dose dependent increase in G2 and S-phases following five days of treatment with MRT67307 and CYT387 in TC71 and TC32 cell lines.

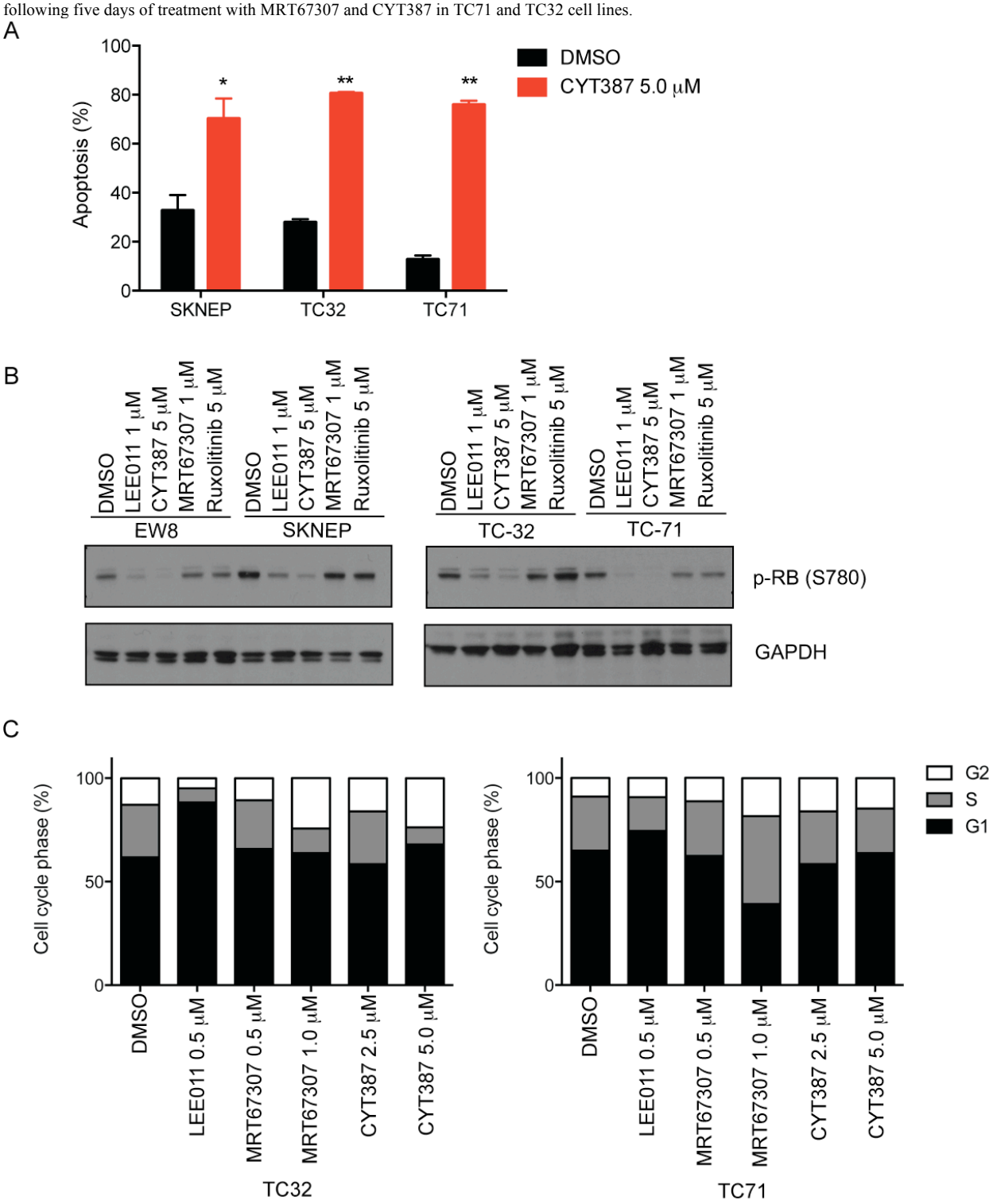

Figure 5: CYT387 attenuates Ewing sarcoma tumor xenograft growth *in vivo* and improves survival. A. Tumor volume was significantly reduced (Student's t-test for each time point, p = 0.036) at day fifteen following treatment with 100 mg/kg of CYT387. Mean tumor volumes are shown +/- SEM. B. Treatment over the course of twenty-nine days also resulted in improvement in survival, p = 0.0231, as calculated by the Mantel-Cox test. There was no difference in the weight of NSG mice over the course of treatment. C. Tumor xenografts of mice treated with CYT387 were harvested at time of sacrifice on day 20 and 27 of treatment and frozen. Protein lysates from tumors show a marginal elevation in p-TBK (S172) suggestive of on-target CYT387activity.

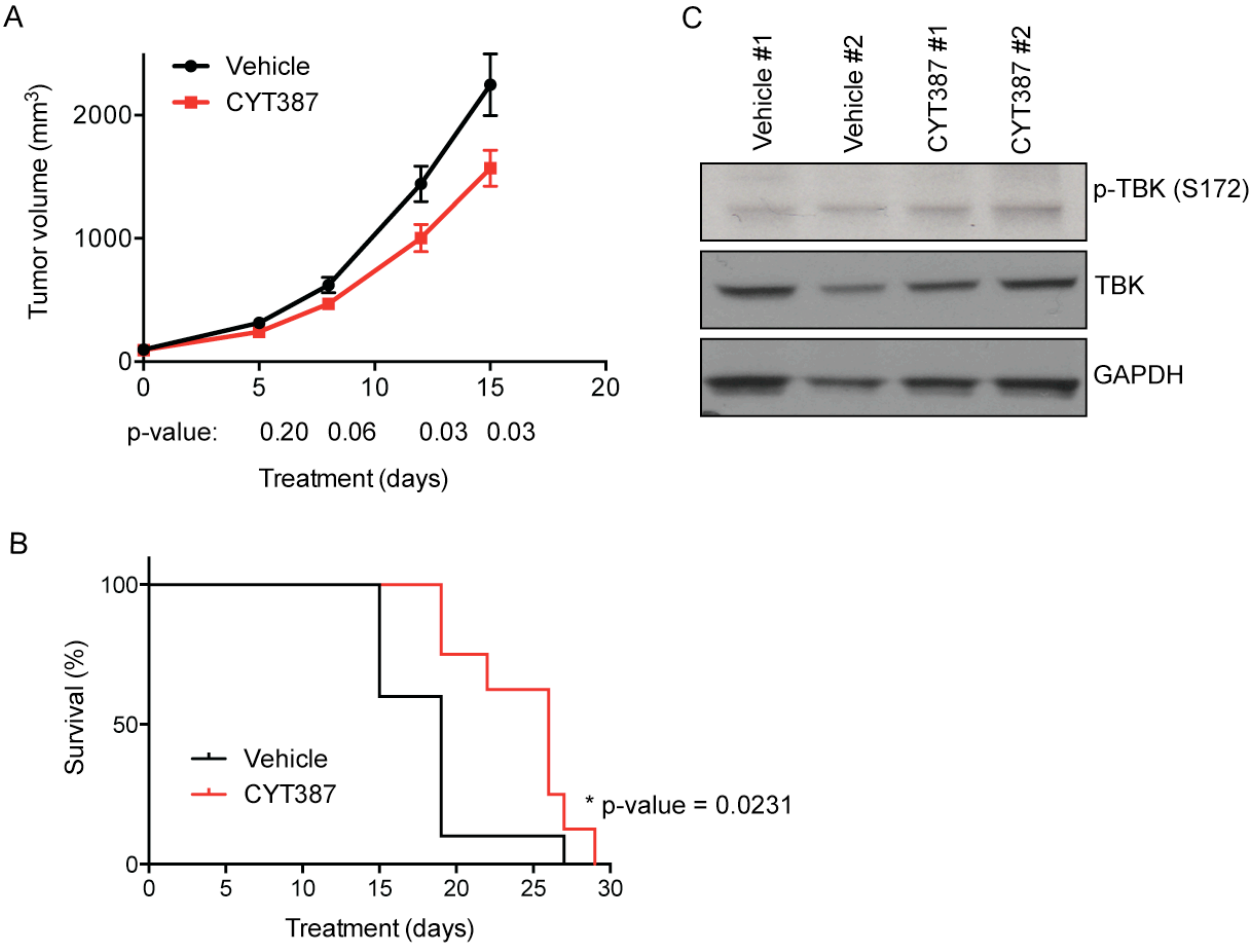

Figure 6: Cyclin D1 and CDK4 score highly in a near whole-genome shRNA screen and are highly expressed in Ewing sarcoma as compared to other tumor types. A. Targeting of CCND1 and CDK4 with shRNAs resulted in significant preferential depletion of Ewing sarcoma cells as compared to non-similar cell lines with hairpins targeting CCND1 and CDK4 scoring in the top ten percent of depleted hairpins. B. Cells expressing EWS/FLI1 have significantly increased sensitivity (p-value 0.033) to the CDK4/6 inhibitor PD-033299. C. RNA sequencing of Ewing sarcoma cell lines shows elevated levels of CCND1 (red) and CDK4 (blue), but not CDK6. This pattern of gene expression parallels expression in a panel of primary patient tumors of which the average expression is shown in the graph below. D. CCND1 and CDK4 are highly expressed in Ewing sarcoma, as measured by mRNA expression, when compared to a panel of other cancer cell lines.

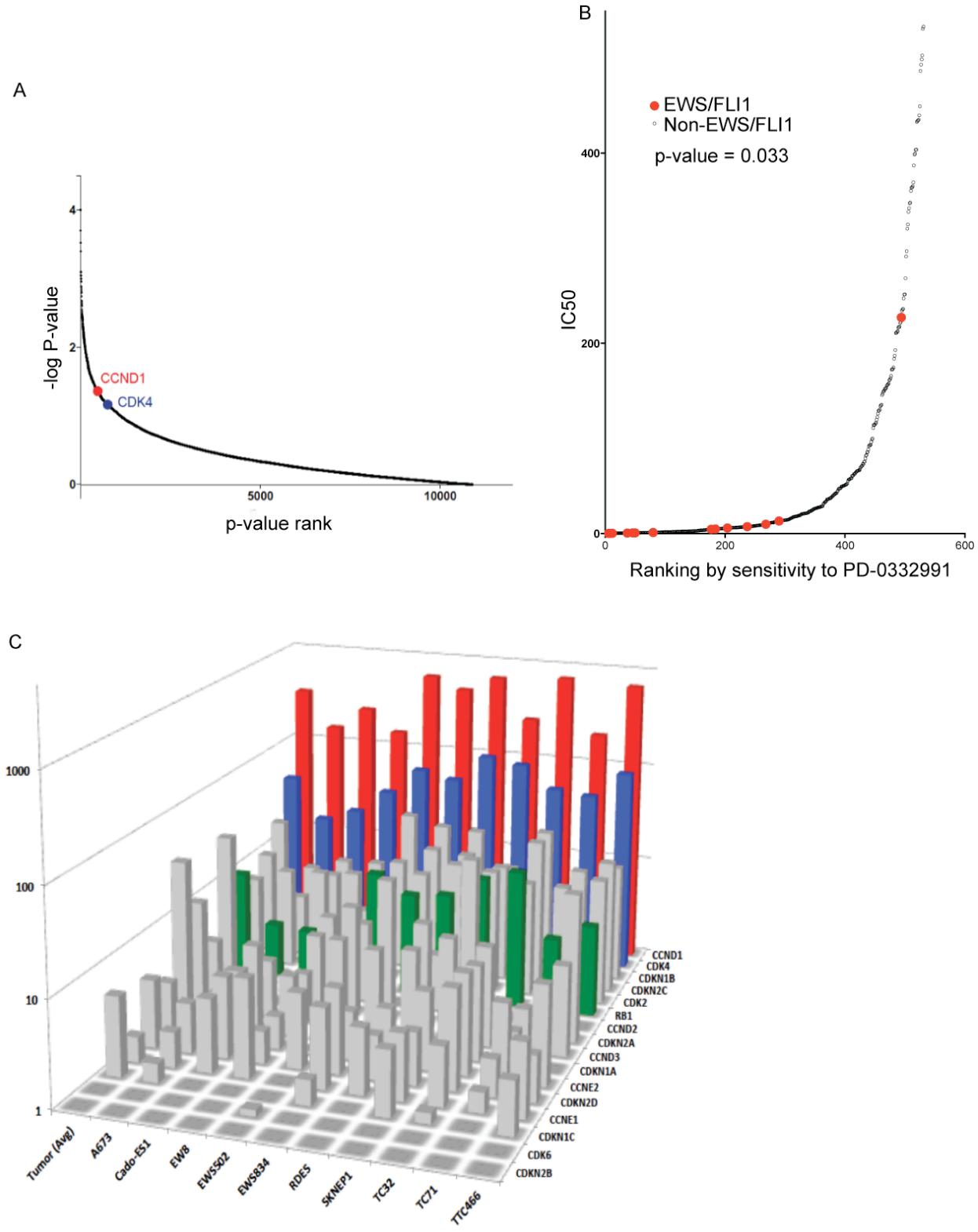

D
CCND1 mRNA level (log2 RNA)
Ewing Sarcoma
Melanoma
Osteosarcoma
Esophagus
Neuroblastoma
Kidney
Meningioma
Prostate
Biliary
Breast
Upper aerodigestive
Urinary tract
Liver
Pancreas
Thyroid
Soft-tissue
Colorectal
Ovary
Stomach
Endometrium
Other
Lung_Non-Small Cell
Mesothelioma
Chondrosarcoma
Glioma
Medulloblastoma
CML
Multiple Myeloma
Hodgkin's Lymphoma
AML
Lymphoma_other
DLBCL
Burkitt's Lymphoma
B-cell ALL
Small cell lung
T-cell ALL
CDK4 mRNA level (log2 RNA)
Neuroblastoma
Ewing Sarcoma
Mesothelioma
Osteosarcoma
Soft-tissue
Colorectal
Burkitt's lymphoma
Endometrium
Meningioma
DLBCL
B-cell ALL
Prostate
Melanoma
Lymphoma_other
AML
Liver
Small cell lung
Kidney
Urinary_tract
Multiple Myeloma
Stomach
Biliary duct
CML
Glioma
Medulloblastoma
Non-small cell lung cancer
Esophagus
Thyroid
Pancreas
Ovary
Breast
T-cell ALL
Other
Hodgkin's lymphoma
Chromdrosarcoma
Upper aerodigestive

Figure 7: Targeting of CDK4 and Cyclin D1 with shRNA mediated knockdown results in impaired cell growth and colony formation. A, B, and C. Panels showing decreased levels of CDK4 after infection of Ewing sarcoma cell lines with three unique shRNAs targeting the transcript, and corresponding impairment in Ewing sarcoma cell growth and anchorage independent growth. D, E, and F. Decreased levels of CCND1 after infection with three unique shRNAs targeting the transcript resulted in downregulation of the protein and impaired cell viability as well as anchorage independent growth. Cell growth was measured using a luminescent ATP detection assay and relative luminescence was calculated by dividing each timepoint's luminescent value by the average day 0 luminescent value for each hairpin. The fold change was calculated in comparison to the hairpin control. Colony formation was performed in methylcellulose and is shown as fold change relative to control shRNA. Shown are the mean of 14 replicates for viability and 2 replicates for colony formation +/- SEM.
(Alyssa Kennedy MD, PhD)

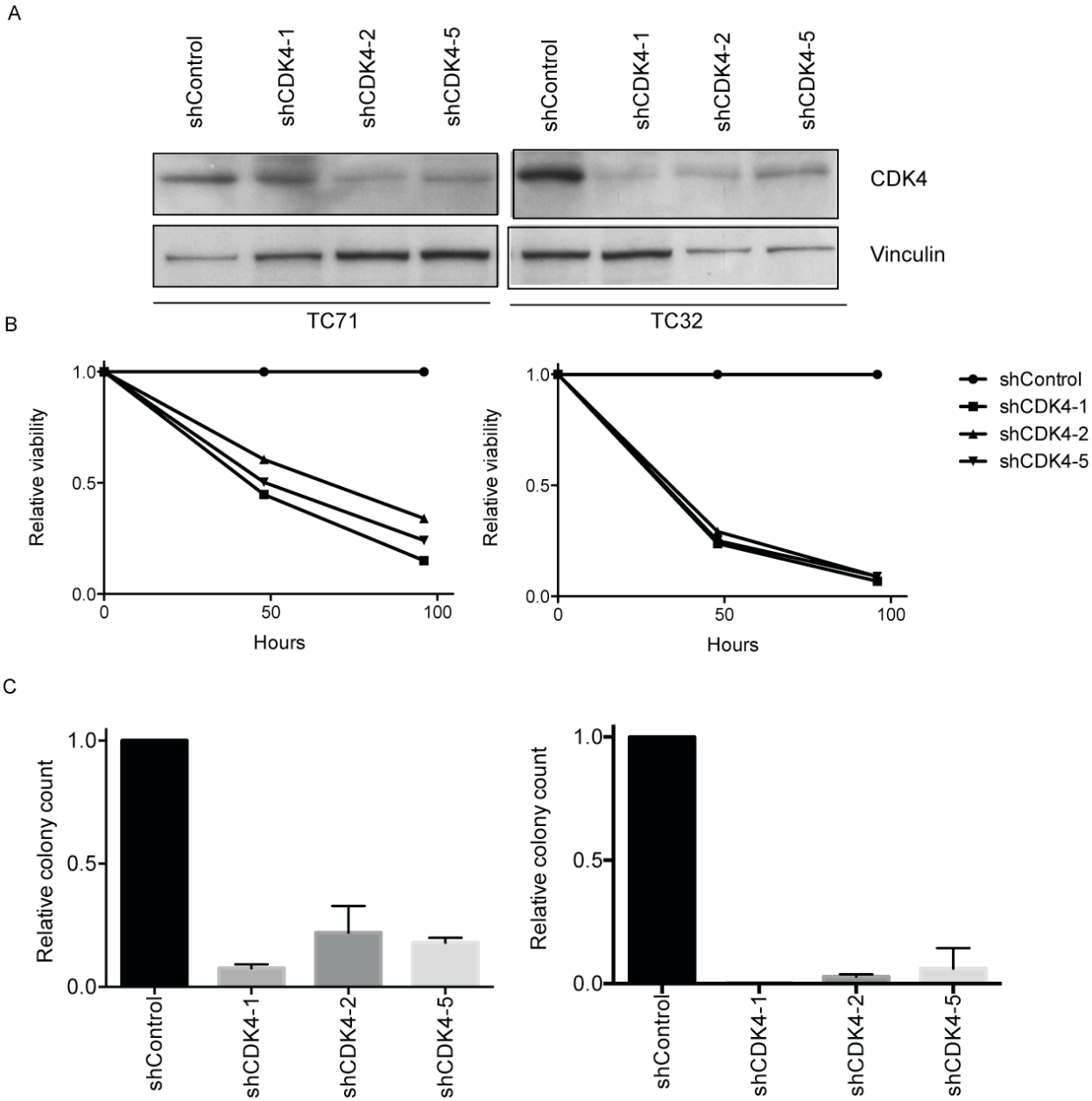

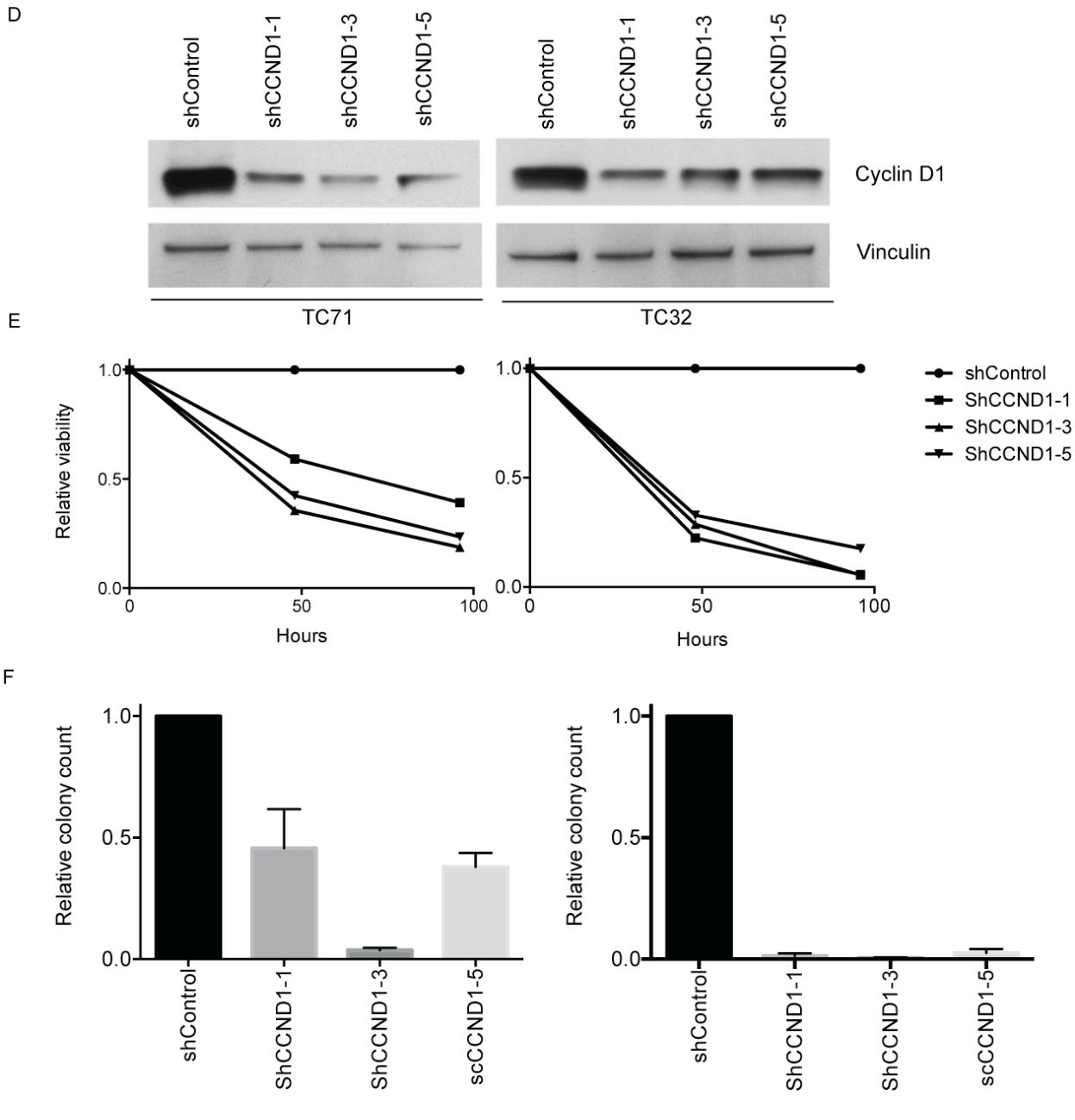
D
shControl
shCCND1-1
shCCND1-3
shCCND1-5
shControl
shCCND1-1
shCCND1-3
shCCND1-5
Cyclin D1
Vinculin
TC71
TC32
E
Relative viability
1.0
0.5
0.0
0
50
100
Hours
1.0
0.5
0.0
0
50
100
Hours
shControl
ShCCND1-1
ShCCND1-3
ShCCND1-5
F
Relative colony count
1.0
0.5
0.0
shControl
ShCCND1-1
ShCCND1-3
scCCND1-5
Relative colony count
1.0
0.5
0.0
shControl
ShCCND1-1
ShCCND1-3
scCCND1-5

Figure 8: Pharmacologic inhibition of CDK4/6 in Ewing sarcoma results in impaired cell viability, G1 arrest and apoptosis in a subset of highly sensitive cell lines. A, B. Effects of five days of treatment with LEE011 (CDK 4,6 inhibitor) on Ewing sarcoma cell viability demonstrates variable sensitivity in the low micromolar range in a panel of Ewing cell lines. C. Treatment along a logarithmic concentration range of LEE011 in eight Ewing cell lines, demonstrates potent G1 arrest at less than 1 μM in sensitive lines and minimal increase in the G1 phase in less sensitive cell lines, TC71 and EW8, following 10 μM concentration for treatment. D. Induction of apoptosis, in addition to cell cycle arrest, following CDK4/6 inhibition is noted in the cell lines with increased sensitivity to LEE011. E. LEE011 demonstrates on-target activity both highly sensitive and less sensitive cell lines with a decrease in phosphorylation of Rb at Serine-780 (S780).

A

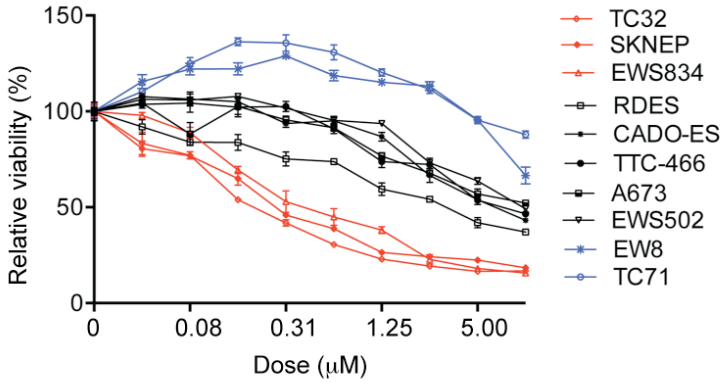

B

Cell Line	IC50 (μM)
TC32	0.26
SKNEP	0.36
EWS834	0.56
RDES	3.19
CADO-ES	6.38
TTC466	6.91
A673	8.63
EWS502	8.67
EW8	11.78
TC71	18.06

C

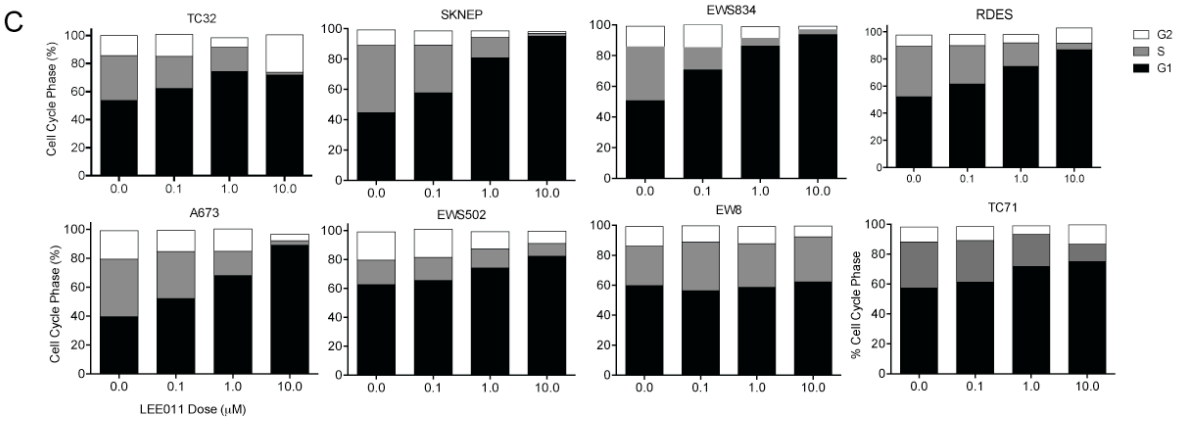

D

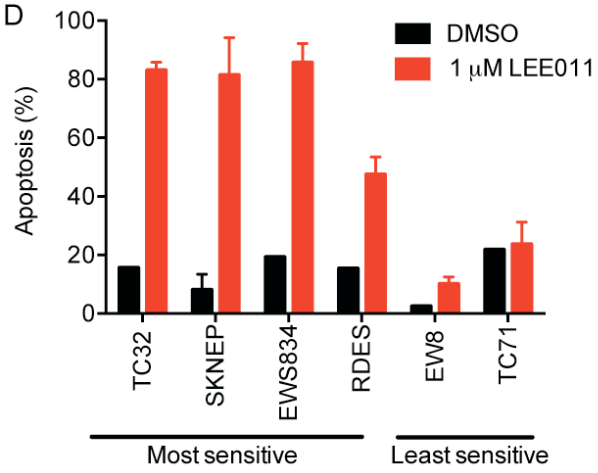

E

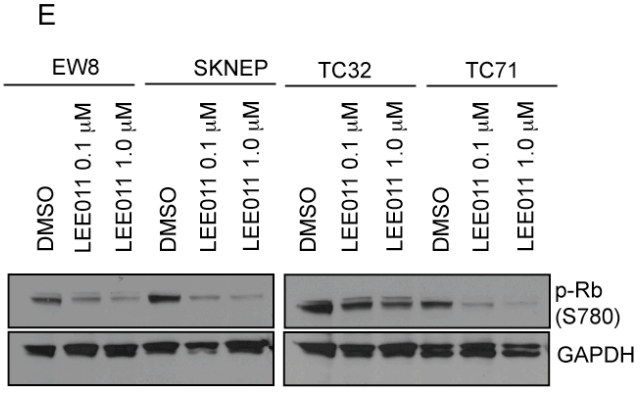

Figure 9: LEE011 impairs Ewing sarcoma tumor xenograft growth *in vivo*. A. Mice treated with LEE011 at 75 mg/kg and 250 mg/kg experienced significantly impaired (Student's t-test for each time point) tumor growth with mild regression of tumor size noted in the highest treatment dose group. B. There was also a modest but significant (Student's t-test for each time point) dose-dependent decrease in relative weight of mice treated with LEE011 over the course of 17 days of treatment, with improvement in weight gain in the 75 mg/kg group following a treatment holiday and supportive care involving hydration and supplemental nutrition.

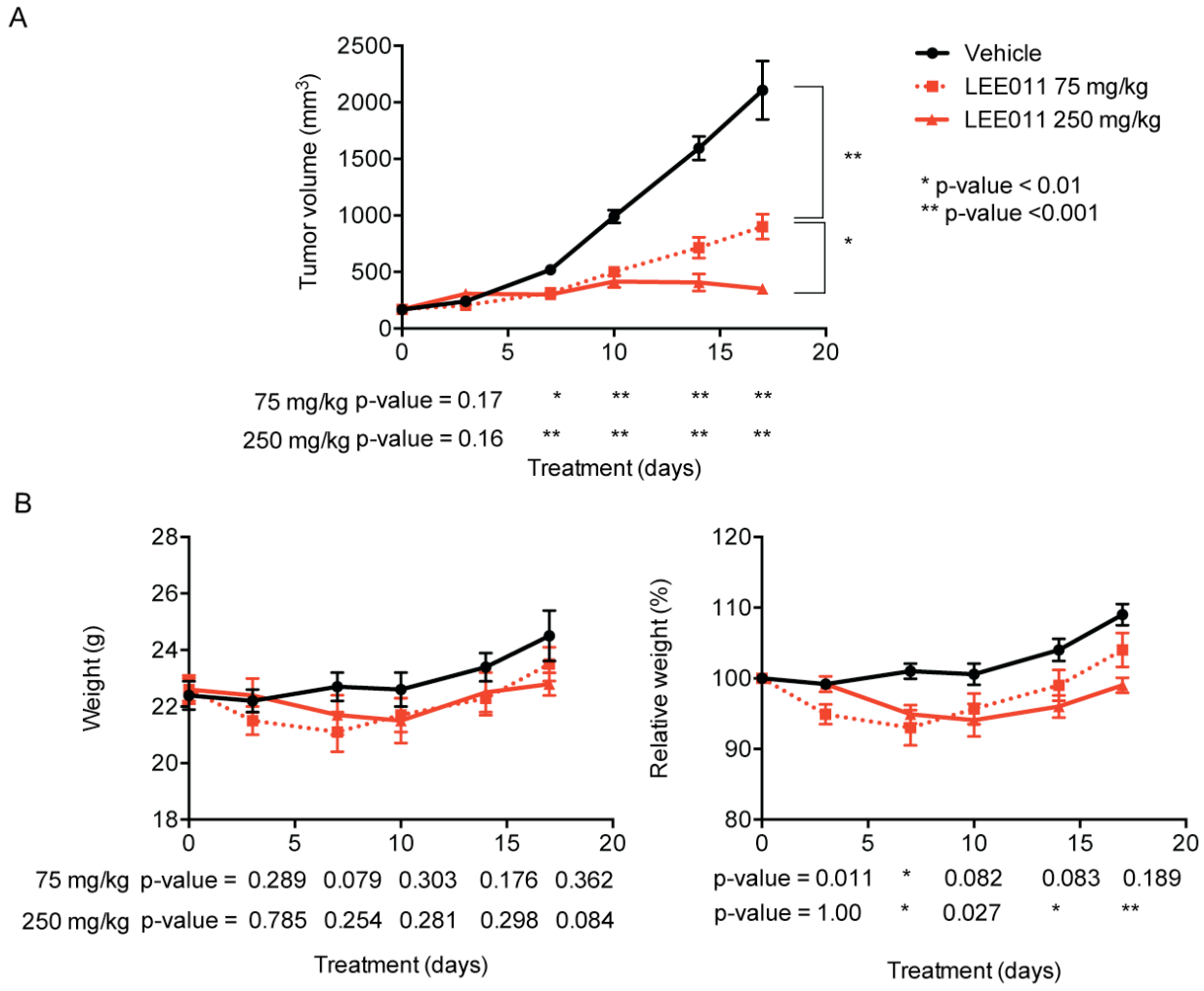

Figure 10: Putative markers of sensitivity to CDK 4/6 inhibition by LEE011. A. We evaluated the association of EWS/FLI1 (EF) or EWS/ERG (EE) expression, as well as EWS/FLI1 fusion type with sensitivity to LEE011. EWS/ERG lines were moderately sensitive to LEE011. Three sensitive EWS/FLI1 lines, SKNEP and RDES had the less prevalent fusion type, type II which involves a fusion between exon 7 of EWS and exon 5 of FLI1 in contrast to the type I fusion which involves exon 7 of EWS and exon 6 of FLI1. EWS834 has neither a type I or II fusion, but a rarer fusion between exon 11 of EWS and exon 8 of FLI1. Despite the prevalence of non-type I fusions in sensitive lines, the most sensitive line to LEE011 has a type I EWS/FLI1 fusion. The loss of CDK2NA (blue) or CDK2NB (blue) did not correlate with sensitivity. Complete data is not available for TTC466 or EW8 as we only have whole exome sequencing (WES) for these lines. TP53 mutations are present in the majority of all Ewing sarcoma lines. B. We evaluated association between Rb and p16 expression and response to LEE011 by comparing RNAseq RPKM values of highly sensitive lines, defined as having sub-micromolar IC_{50}'s, with the less sensitive lines and noted a significant decrease in Rb expression in the less sensitive lines. However there is also a great deal of variability in Rb expression amongst the highly sensitive lines. Expression of p16 did not correlate with sensitivity. C. The expression of cyclin D1b, the oncogenic isoform of Cyclin D1 has variable expression across Ewing cell lines, with a decreased ratio of cyclin D1b to cyclin D1a in cell lines with increased sensitivity to CDK4 inhibition, (highest sensitivity lines marked with red asterisk).

A

	TC32	SKNEP	EWS834	RDES	CADO-ES	TTC466	A673	EWS502	EW8	TC71
IC50 (μM):	0.26	0.36	0.56	3.19	6.38	6.91	8.63	8.67	11.78	18.06
Fusion:	EF	EF	EF	EF	EE	EE	EF	EF	EF	EF
Fusion type:	I	II	Not I or II	II	N/A	N/A	I	I	I	I
CDKN2A						WES			WES	
CDKN2B						WES			WES	
TP53		p.G245S	p.R249M	p.R273C		p.R175H	p.T118fs	p.C135F	p.Y220C	p.R213*

B

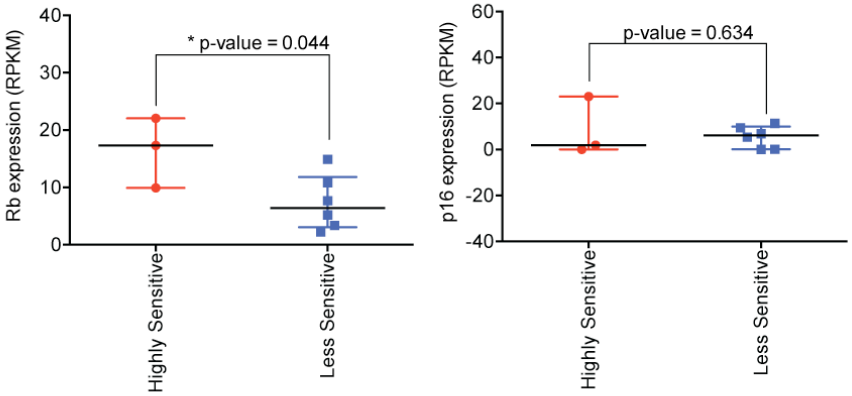

C

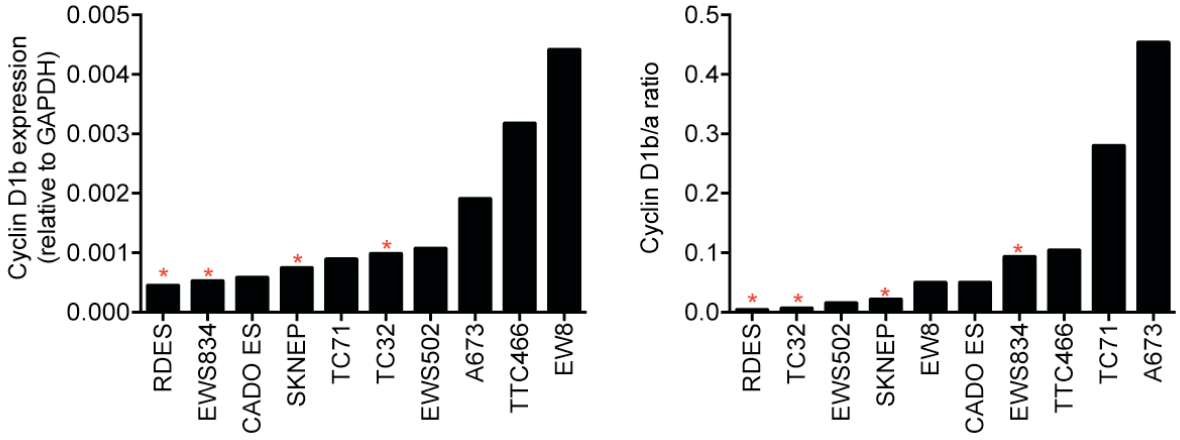

Supplemental Figure 1: Suppression of a highly homologous protein to IKBKE, TBK1, impairs cell growth and colony formation. A. Western immunoblots of protein lysates from Ewing sarcoma cell lines infected with three unique shRNAs targeting the TBK1 transcript, and resultant suppression of protein expression. B, Suppression of TBK1 protein results in impaired cell growth. Cell growth was measured using a luminescent ATP detection assay and relative luminescence was calculated by dividing each days luminescent value from the average day 0 luminescent value for each hairpin. C. TBK1 knockdown impairs colony formation. Colony formation in methylcellulose relative to control shRNA. Shown are the mean of 14 replicates for viability and 2 replicates for colony formation +/-SEM.

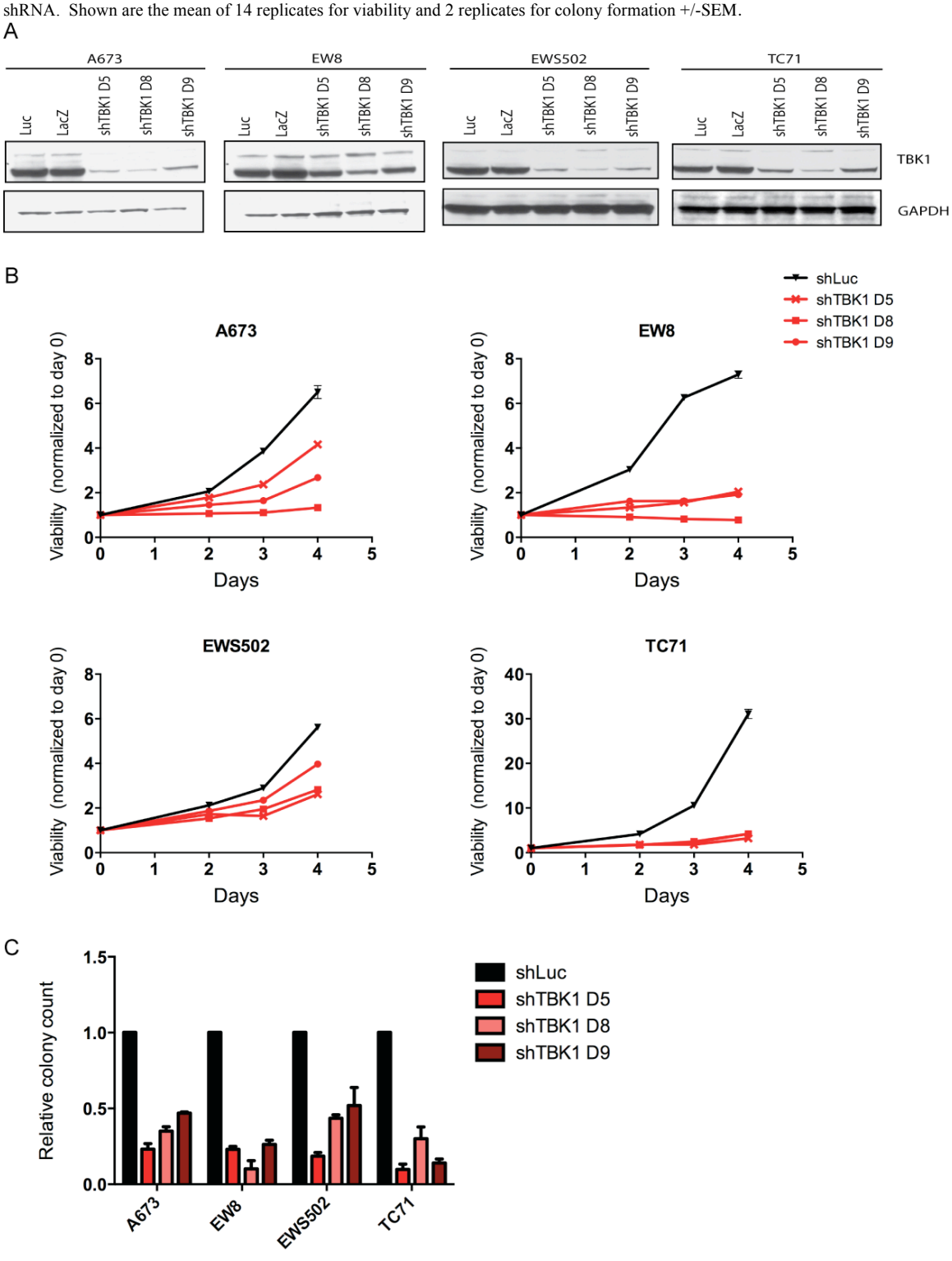

Supplemental Table 1: Top 100 essentiality gene hits based on Ewing non-specific and Ewing specific scores. Genes are ranked based on the p-values assigned by the weighted sum of two hairpins method implemented in RIGER.

#	Ewing non-specific	Ewing vs all non-Ewing	Ewing vs least Ewing-like
1	APOBEC3F	STRN4	RASL10B
2	RPS7	PDXP	CKLF
3	SNRPE	S100A10	STRN4
4	RAN	SHPRH	PDXP
5	RPS13	MINK1	S100A10
6	RPL23A	PPP1R1A	BIRC2
7	EIF2S2	BIRC2	IDH1
8	RPS15A	LATS2	BHLHE41
9	NHP2L1	AXL	PPP2R4
10	GRIK1	CKLF	PCDHB3
11	PCBP2	CTH	HSD17B1
12	RPS27A	BHLHE41	KCND2
13	PSMD11	DCLRE1B	MINK1
14	PSMB2	NEURL	SPR
15	PSMD1	APEX2	CTH
16	NUP93	TRERF1	RFPL1
17	WDR86	GGA2	PCDHA10
18	NCOR2	DSG2	ADAMTS4
19	EFTUD2	CD99	LATS2
20	ZNF439	RFPL1	SHPRH
21	EIF1AX	PCDHB3	PPP1R1A
22	PSMA1	IKBKE	ISG20
23	ZNRF2	IL2RG	CIAO1
24	RPS4X	RASL10B	CAMK4
25	LSM6	KCND2	YKT6
26	EIF6	FECH	APEX2
27	SNRNP200	PCDHA10	DSG2
28	BAP1	RHBDD2	KATNA1
29	KCNJ5	ZNF234	CD3E
30	SNRPD2	IDH1	IL2RG
31	NCBP1	SPR	FECH
32	RPS29	AP1M1	C5orf45
33	RPS9	SRXN1	BCKDHB
34	EIF5B	WNT10B	TAF7
35	GREM1	CD8A	HERC1
36	LSM3	C5orf45	SCN1A
37	HNRNPU	HIST1H2BL	FKRP
38	PRPF19	BAP1	ZNF234
39	PAQR6	AK7	PAX7
40	RPS8	LYVE1	ABAT
41	TAF7	VANGL1	APLP2
42	RPS6	U2AF1L4	BATF

43	RPL6	GFRA3	AK7
44	INPP5F	CD302	NUDT13
45	RABEP1	PLS1	NEURL
46	RPS19	PPP2R4	DCLRE1B
47	SNRPG	SLC1A2	SRXN1
48	DDX46	FKRP	C4A
49	ARCN1	KRT28	WNT10B
50	OSCAR	MYL9	ZNF646
51	CD82	BCKDHB	VANGL1
52	LSM5	UQCRFS1	GFRA3
53	N4BP2	HIST1H2BC	AGPAT3
54	TAF4B	C4A	TCN2
55	RPL32	RAB3A	ABCF2
56	EIF3A	APLP2	AKAP10
57	SF3B5	ITGB2	GGA2
58	ADCYAP1R1	AVPR2	ESRRA
59	ABHD12	KIF12	LTBR
60	TBC1D25	CAMK4	ITGB7
61	RPS18	AGPAT3	SMAD4
62	CDC5L	MECP2	KRT28
63	POLA1	PRKACB	SGIP1
64	DDX19B	TCN2	SLC1A2
65	RUVBL2	ESRRA	HPS3
66	HNRNPC	CIAO1	CD99
67	MSR1	HSD17B1	AXL
68	VPS29	HNRNPH1	AGTR2
69	ERCC6L	SATL1	COX4I1
70	TMC7	UCHL3	AP1M1
71	U2AF1	N6AMT1	LYVE1
72	ACTL6A	RTCD1	DFNA5
73	FECH	TCAP	U2AF1L4
74	NCL	DFNA5	RHBDD2
75	RPS14	SGIP1	UBE2L6
76	RPL7	RPS6KA2	SSBP4
77	ZBTB40	BATF	N6AMT1
78	EIF4A3	NUDT13	CD180
79	RNF139	SLC15A3	IMPACT
80	HAL	CD3E	UCHL3
81	WBP11	ARHGEF1	SATL1
82	TIAL1	NECAB2	CD8A
83	PRKDC	EPHB1	SLC7A3
84	AFAP1L1	ABCF2	PLK4
85	ACYP2	KCNJ11	IKBKE
86	RPS17	PRSS21	CAPS
87	UBB	IMPACT	MXRA5
88	PRPF3	PFKFB4	RTCD1
89	CAT	FAM64A	HIST1H2BL

90	APOL2	COX4I1	HOXC6
91	DNAJB2	SCN1A	FABP7
92	ISL1	ATF6B	DOCK1
93	POLR2D	PDE4DIP	HGF
94	EFCAB11	CD180	WSB2
95	ZNF222	PREX1	OPRD1
96	RBM17	LPCAT2	IRF5
97	PSMB6	FGG	AGPS
98	GRIN1	ICOSLG	ZNF212
99	SUPT6H	SNX27	TRERF1
100	EIF3H	EEF1D	TAF9B

Supplemental Table 2: List of pLKO.1 shRNA sequences targeting IKBKE, TBK1, CDK4, CCND1

	Clone ID	**Target Sequence**
shControl		CCTAAGGTTAAGTCGCCCTCGC
shLuc	TRCN0000072253	ACACTCGGATATTTGATATGT
shIKBKE-3	TRCN0000010036	TGGGCAGGAGCTAATGTTTCG
shIKBKE-5	TRCN0000010027	GAGCATTGGAGTGACCTTGTA
shIKBKE-35	TRCN0000010035	TGCCCACAACACGATAGCCAT
shTBK1 D5	TRCN0000003182	GCAGAACGTAGATTAGCTTAT
shTBK1 D8	TRCN0000003185	GCGGCAGAGTTAGGTGAAATT
shTBK1 D9	TRCN0000003186	CGGGAACCTCTGAATACCATA
shCDK4-1	TRCN0000000364	GAAATTGGTGTCGGTGCCTAT
shCDK4-3	TRCN0000000362	ACAGTTCGTGAGGTGGCTTTA
shCDK4-5	TRCN0000197041	CTCTGAGAGGGCAATCTTT
shCCND1-1	TRCN0000040038	GCCAGGATGATAAGTTCCTTT
shCCND1-2	TRCN0000040042	GAACAAACAGATCATCCGCAA
shCCND1-5	TRCN0000010317	GATTGGAATAGCTTCTGGAAT